Progress in Organic Coatings 193 (2024) 108541

Contents lists available at ScienceDirect

Progress in Organic Coatings

journal homepage: www.elsevier.com/locate/porgcoat

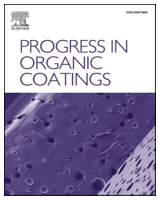

Preparation of high-solid PLA waterborne dispersions with PEG-PLA-PEG block copolymer as surfactant and their use as hydrophobic coating on paper

Matteo Calosi [a], Andrea D'Iorio [a], Elena Buratti [a], Rita Cortesi [a], Silvia Franco [b], Roberta Angelini [b], Monica Bertoldo [a,*]

[a] Department of Chemical, Pharmaceutical and Agricultural Sciences, University of Ferrara, via. L. Borsari, 46, 44121, Ferrara, Italy
[b] Institute for Complex Systems, National Research Council (CNR-ISC), Piazzale A. Moro 2, 00185, Rome, Italy

ARTICLE INFO

Keywords:
Poly(lactic acid)
Coatings
Waterborne
Paper

ABSTRACT

Paper-based packaging is experiencing a resurgence due to its inherent biodegradability and recyclability. To meet the barrier properties required for certain applications, a coating is necessary. This coating must enhance functionality without compromising the environmental sustainability of the substrate. With this goal in mind, we prepared waterborne dispersions of biodegradable poly(lactic acid) (PLA) using a PEG-PLA-PEG triblock copolymer as the main surfactant. We achieved formulations with good stability over a 6-month period and high solids content (~40 wt%). The waterborne dispersions underwent analysis by dynamic light scattering (DLS), size exclusion chromatography (SEC), gravimetric tests, and rotational rheology with and without xanthan gum (0.2–0.8 wt%) as a thickener. Subsequently, the thickened dispersions were coated at 60 °C onto a paper substrate. SEM analyses revealed the formation of a polymer layer on the paper surface with thickness and morphology dependent on the processing conditions. Partial interpenetration between the coating and the paper fibers was observed, resulting in excellent adhesion between the layers. The coated paper exhibited good barriers to liquid and water vapor, with Cobb60 < 5 g/m^2 and water vapor transmission rate (WVTR) < 100 g/(m^2•day) for coating weights ≤ 15 g/m^2, comparable to the performance of solvent-based PLA paper coatings. The surface energy of the coating was approximately 50 dyne/cm, higher than that of neat PLA, making it suitable for printing with common inks. Furthermore, the coated paper can be fully pulped in water, indicating that it can still be recycled in the paper stream, albeit with potentially increased processing time due to the coating weight.

1. Introduction

Paper-based packaging is experiencing a resurgence, driven by bans on single-use plastics and consumer preference for paper over plastic packages, leading the industry to prioritize paper whenever feasible due to its inherent biodegradability and recyclability [1,2]. Since paper itself is hydrophilic and porous, with poor barrier properties and low resistance to water and grease, it is often coated or treated to enhance its properties. The most commonly used coatings are petroleum-based polymers such as polyethylene (PE), poly(vinyl chloride) (PVC), ethylene vinyl alcohol (EVOH) and others depending on the application. However, these materials raise environmental and health concerns due to their lack of biodegradability, potential release of dangerous substances (e.g., microplastics or polyfluoroalkyl substances), use of volatile organic compounds (VOCs) during application, and limitations to the recyclability of the final paper product [3–5].

Two of the most important developments in the coating industry in recent decades have been the shift towards bio-based and biodegradable coatings, replacing classic fossil-based non-biodegradable polymers, and the increasing use of water-based technologies for coating application as alternatives to extrusion coating and solvent-based methods.

Various biodegradable alternatives to fossil-based polymers are used for coating purposes. Natural biopolymers such as polysaccharides (e.g., starch, chitosan, modified cellulose) or proteins (e.g., zein) have been widely tested, but they often encounter limitations due to their inherent hydrophilicity, which restricts their water barrier and resistance properties [3,6]. More desirable barrier properties can often be achieved by coating with biodegradable aliphatic polyesters such as

* Corresponding author.
E-mail address: monica.bertoldo@unife.it (M. Bertoldo).

https://doi.org/10.1016/j.porgcoat.2024.108541
Received 8 April 2024; Received in revised form 16 May 2024; Accepted 25 May 2024
Available online 31 May 2024

polyhydroxyalkanoates (PHAs), polycaprolactone (PCL), poly(butylene-succinate) (PBS), and poly(lactic acid) (PLA), which exhibit significantly higher hydrophobicity [7].

PLA, in particular, can be considered a moderately hydrophobic material, as it is water-insoluble and has a surface contact angle with water of 65–80°. However, it possesses poor gas barrier properties against both water vapor and oxygen compared to many fossil-based polymers [8–10]. At present, PLA is most intriguing in the paper coating field for reducing water absorptiveness and thus increasing resistance to humidity, rather than as barrier packaging [11,12] although many potentially interesting PLA composites with improved barrier properties are being tested [13]. PLA undergoes slow biodegradation when dispersed in the environment, but it is fully degradable under appropriate composting conditions [14].

The recyclability of coated paper is a separate issue from its biodegradability. Coating biodegradability does not affect the paper recycling industry, as "rejects" from the repulping process are not separable and are disposed of together. In general, the lower the coating weight, the more recyclable the coated paper will be, although there is no universal coating weight value above which paper is no longer recyclable. Current guidelines, such as those from the UK Confederation of Paper Industries, recommend that coating weight should not exceed 10 % of the total pack weight and aspire to reach 5 % in the future [15]. Thus, minimizing the amount of coating weight, apart from the general advantages of using less plastic, is also preferable for paper recycling purposes. Nevertheless, the biodegradability of paper used for packaging remains an important factor, reducing environmental impact in case of improper disposal or littering, as well as allowing for the compostability of food-contaminated packaging.

The most common technique for obtaining polymer-coated paper is extrusion coating. However, this method has limitations in producing films with minimum thicknesses depending on the polymer melt strength. While thicknesses down to 10–15 μm may be achieved with PE films, this is not feasible with most bio-based polymers like PLA or PHAs (minimum thicknesses of 20–30 μm) due to their lower melt strengths [16]. Adhesion to the paper substrate is also reduced when thinner films are extruded [17]. These issues are mitigated with "wet" methods, which allow the production of very thin coatings by depositing polymers on the paper substrate dissolved or dispersed in a liquid phase, which is then evaporated. However, organic solvent-based coatings contribute to high consumption of volatile organic compounds (VOCs), with adverse effects on the environment and health. Therefore, water is preferred as a non-toxic and environmentally sustainable solvent for coatings, but most polymers, especially hydrophobic ones, are insoluble in water.

The polymers most commonly applied as paper coatings via water-based technologies are currently obtained from radically polymerizable fossil-based monomers such as styrene and acrylates by directly polymerizing in emulsion, thus obtaining high-solid content formulations [18,19]. However, this route is not available for polyesters and biodegradable polymers in general, which need to be dispersed in the aqueous phase after synthesis. To be of industrial interest, the water-borne formulations obtained need to fulfill several requirements: stability over time, high (> 40 %) solid content, and ease of application. Interest in obtaining these formulations is increasing, as evidenced by recent examples using PBS [20] and PHAs [21].

PLA waterborne formulations have been the most researched among the various biodegradable polyesters. At the time of writing, a commercial PLA waterborne product line exists, sold by Miyoshi Oil & Fat Co. (Tokyo, Japan) [22]. These formulations have a particle size between 1 and 5 μm, 40 % solid content, and are sold for adhesive and paper coating applications. Industrial research is active on this subject, as evident from patent literature. For example, recent publicly available patents describe formulations of waterborne PLA using low-molecular-weight plasticizers as dispersants for cosmetic use [23], and formulations using poly(vinyl alcohol) (PVA) in combination with polymeric surfactants and thickener [24].

Scientific literature has been lagging behind industrial research, with the first high-solid stable PLA latex (a composite containing montmorillonite with 25 wt% solid content) being reported in 2016 by Bandera and colleagues [25]. This was tested as paper coating and showed an 85 % reduction in water vapor transmission rate (WVTR) compared to the original paper at a coating weight of 20 g/m^2. Our research group more recently tested the stability and filmability of waterborne dispersions of PLA, finding a range of ionic and non-ionic surfactants that were able to form stable dispersions [26]. We then measured the rheological properties of such dispersions using xanthan gum (XG) as a thickener to obtain a formulation more easily usable for coating and paint applications compared to the original dispersions [27]. We also used waterborne PLA dispersions to achieve blends of this polymer with PVA [28]. Most recently, Abdenour and colleagues [29] reported the properties of paper coated using XG-thickened aqueous PLA dispersions using commercial non-ionic surfactants. This formulation was intentionally low-solid (3–4 wt%) to limit the volume of organic solvents used per volume of water, and a reduction in WVTR above 90 % was obtained at a coating weight of 15 g/m^2, while water absorption was not tested.

The PLA used for coatings may be amorphous or semi-crystalline, with the degree of crystallinity depending on the quantity of D-lactide used in the polymerization. While semi-crystalline PLA confers materials with more desirable mechanical properties, its solubility in organic solvents is more limited. The most commonly used solvents are chlorinated solvents such as dichloromethane and chloroform, which are toxic and environmentally harmful. Amorphous PLA, on the other hand, is readily soluble in a wider array of solvents, allowing for the use of greener alternatives such as ethyl acetate [30].

In our group's previous research [26], we found that Synperonic PE/F68, a commercial poly(ethylene glycol)-*b*-poly(propylene glycol)-*b*-poly(ethylene glycol) (PEG-PPG-PEG) triblock copolymer by Croda, was an effective surfactant for forming waterborne dispersions of PLA. In this work, we aim to improve on the properties of these dispersions by synthesizing and using a structurally analogous PEG-PLA-PEG triblock copolymer, in which PLA serves as the hydrophobic component of the surfactant in place of PPG. The hydrophilic-lipophilic balance (HLB) of the block copolymer was aimed to be similar to that of the commercial product by using a similar overall ratio between the hydrophilic PEG component and the hydrophobic PLA component.

PLA-PEG block copolymers have been reported since the late 1980s [31,32], and, since then, they have been extensively used in drug delivery research due to their biocompatibility and easy functionalization, making them versatile drug carriers [33]. However, very little research has been conducted on the use of these copolymers outside the biomedical field, although in recent years, they have been reported as possible plasticizers for PLA [34], as well as crystallization and toughness enhancers [35].

Our aim in this work is thus to use these copolymers as surfactants, with the ultimate purpose of obtaining stable waterborne dispersions of PLA with high solid content, and to study their use in coating applications. To achieve this, we used the oil-in-water methodology from our previous work, characterized the resulting dispersions, and assessed their stability over time. We also evaluated the filmability of the samples, the level of plasticization conferred by the surfactant, and the consequent changes in film -forming temperature. Different formulations were prepared to find the optimal surfactant content to achieve long-term (> 6 months) stable dispersions with minimal phase separation. We also analyzed the hydrolytic stability of PLA itself when stored as a waterborne dispersion at 4 °C, an aspect for which there is little reference, as PLA hydrolysis research has mostly focused on the accelerated degradation of the polymer at higher temperatures (≥ 37 °C) [36–38].

Concentration by water evaporation was used to maximize the solid content of the dispersions, as far as these could be kept stable. XG was then used to thicken the PLA dispersion and allow its use for paper coating through hand coater application on a heated surface. The

resulting coated paper was studied using scanning electron microscopy (SEM), and its barrier properties against liquid water and water vapor were assessed by measuring water absorptiveness and water vapor transmission rate (WVTR). To ensure the recyclability of coated paper, we aimed to minimize coating weight by optimizing the coating formulation and application process and studied the repulpability of samples at different coating weights.

2. Materials and methods

2.1. Materials

Poly(lactic acid) Ingeo PLA 4060D (PLA) was kindly provided by NatureWorks LLC (Minnetonka, MN). PLA 4060D is an amorphous polymer with an L-lactide content of around 88 wt%. Xanthan gum Satiaxane CX2QD (XG) was supplied by Cargill Deutschland GmbH (Krefeld, Germany). Methoxypolyethyleneglycol (mPEG), with a nominal average molecular weight ($\overline{M_n}$) of 2 and 5 kDa and a dispersity index of 1.06, L-lactide, sodium dodecyl sulfate (SDS), hexamethylene diisocyanate (HDI), and 4 Å molecular sieves were purchased from Sigma-Aldrich (St. Louis, MO). Stannous octoate ($Sn(Oct)_2$) and acid red 87 were purchased from TCI Chemicals (Tokyo, Japan). Analytical-grade solvents (toluene, ethyl acetate, dichloromethane, diethyl ether) as well as HPLC-grade solvents (chloroform) were purchased from Carlo Erba (Milan, Italy). mPEG was dehydrated by azeotropic distillation under nitrogen flow using anhydrous toluene and a Dean-Stark apparatus and then dried under reduced pressure before use. Anhydrous toluene and ethyl acetate were obtained by storing the solvent for at least 3 days and no more than a month over 20 % weight/volume (wt/v) of 4 Å molecular sieves, activated by 200 °C heating for a day. L-lactide was recrystallized twice from anhydrous ethyl acetate, dried under vacuum, and stored under nitrogen. Ultrapure water was obtained using a Sartorius Arium® Mini (Sartorius Lab Instruments GmbH & Co. KG, Göttingen, Germany) water purification system fed with pretreated deionized water. Standard printing paper (Copy paper, Indonesia) used for coating had a thickness of 98 ± 2 μm, a grammage of 71 ± 1 g/m^2, and a water absorptiveness of 100 ± 10 g/m^2 as measured by the Cobb60 test.

2.2. Synthesis of mPEG-PLA-mPEG block copolymers (ELE)

15.010 g of mPEG (7.51 mmol), 3.000 g of L-lactide (20.83 mmol), and 45 mL of anhydrous toluene were heated to reflux under a dry nitrogen atmosphere, and 0.12 g of $Sn(Oct)_2$ (0.3 mmol) was then added. After 24 h, the reaction mixture was cooled to 60 °C, and 0.600 g (3.57 mmol) of HDI was added dropwise. After leaving the reaction overnight, 0.100 g (0.43 mmol) of HDI was further added in 20 mg increments until no further reduction in the dispersity value by GPC-SEC was noticed. The mixture was cooled to room temperature and precipitated twice into diethyl ether. The precipitate was finally dried under reduced pressure (0.2 mbar) until a constant weight was reached. 16.983 g of product was obtained (91 % yield).

2.3. Preparation of aqueous dispersions of PLA

3.740 g of PLA was dissolved in 34 mL of ethyl acetate at 50 °C, and the appropriate weight of surfactants (ELE from 0.260 to 0.780 g and SDS from 0 to 0.520 g) was dissolved into 26 mL of ultrapure water. The organic phase was added to the aqueous phase in a 100 mL glass beaker at room temperature and homogenized at 0 °C using a Hielscher UP200St ultrasonicator (Hielscher Ultrasonics, Teltow, Germany) equipped with a 14 mm diameter probe, set at 50 % intensity for 30 s and then at 80 % intensity for 90 s. The resulting emulsions were mechanically stirred under a fume hood for at least 18 h or until complete removal of the organic solvent. The PLA dispersions were stored at 4 °C. To obtain high-solid aqueous dispersions of PLA, the necessary water was removed from the originally prepared aqueous dispersions using a rotary evaporator set at 40 °C, periodically weighing the sample until the overall weight was in the desired range.

2.4. Characterization of aqueous dispersions of PLA

The solid content of PLA dispersions was measured by comparing the original weight of a 200–400 mg sample with the same sample after heating for 3 h at 150 °C. Dispersions were manually shaken for 10 s prior to sampling. Dynamic light scattering (DLS) measurements were carried out using a Malvern Zetasizer Nano S90 (Malvern Panalytical, Malvern, UK). Samples were diluted to approximately 0.1 mg/mL of PLA using ultrapure water. Measures were carried out in triplicate at 25 °C, and an average result correlogram was generated using Zetasizer 8.02 software. The Z-average diameter derived from this average correlogram was generally reported as particle diameter. Intensity size distribution was generated by the same software using the non-negative least squares (NNLS) inversion method.

The Z-potential of the dispersions was determined by phase analysis light scattering (PALS) at 25 °C using a NanoBrook Omni Particle Size Analyzer (Brookhaven Instruments Corporation, Holtsville, USA) equipped with a 35 mW red diode laser (nominal 640 nm wavelength). The analyses were carried out on samples at ~0.25 wt%, and the reported data are the average over five repeated measurements, with the standard deviation between measurements taken as the uncertainty value.

Size-exclusion chromatography (SEC) analyses were performed with an instrument set comprised of a Jasco PU-4180 pump (JASCO Corporation, Tokyo, Japan) operating at 0.4 mL/min, two in-series PLgel miniMIXED-D columns (Agilent, Santa Clara, USA), a Jasco CO-4060 column oven, a 20 μL injector, a Jasco RI-4030 refractive index detector, and a Jasco UV-4075 multi-channel UV–Vis detector. The column oven was set at 30 °C, and the eluent used was HPLC-grade chloroform. Polystyrene standards were used for calibration.

^{1}H Nuclear Magnetic Resonance (NMR) measurements were carried out on a Varian Mercury Plus 400 (Varian Inc., Palo Alto, USA) equipped with an Oxford NMR AS400 MHz autosampler (Oxford Instruments, Abingdon, UK) at room temperature. The sample concentration was approximately 30 g/L. Chemical shifts were referred to TMS as the external standard by using the solvent peak as the internal standard.

PLA films were obtained by pouring 3 g of dispersion into a Petri dish (⌀ 55 mm) and drying for 2 h at 60 °C in an oven, while covering the dish with filter paper to slow down evaporation and avoid surface cracking.

MFFT was measured by pouring 200 μL of dispersion on an aluminum plate that was pre-heated and kept at the desired temperature for 20 min while observing the film formation. Tests were performed at 1 °C intervals, and the MFFT was considered as the minimum temperature at which a mostly transparent and continuous film to the naked eye was obtained, as opposed to a white and heavily cracked one.

DSC measurements were carried out on a PerkinElmer DSC 8000 calorimeter equipped with an IntraCooler II cooling device (PerkinElmer Inc., Shelton, USA). 5–7 mg of sample in an aluminum open pan was first heated up from room temperature to 240 °C, held isothermally for 5 min, cooled down to −60 °C, held isothermally for 5 min, and heated up again up to 240 °C. Heating and cooling steps were performed at 10 °C/min.

Rheological measurements were performed with a rotational rheometer Anton Paar MCR 102 (Anton Paar Group AG, Graz, Austria) equipped with a cone-plate geometry (plate diameter = 24.964 mm, cone angle = 1.998°, truncation = 104 μm) and a Peltier temperature controlling unit to keep the temperature constant at T = 25 °C. An evaporation control system, and an isolation hood prevented solvent evaporation and sample drying. Flow curves were measured in the shear rate range $\dot{\gamma}$ = (10^{-1}–10^{4}) s^{-1}. A pre-shear of $\dot{\gamma}$ = 100 s^{-1} for 60 s,

followed by a rest of 300 s before each measurement, was applied to erase any mechanical history. The experimental curves were obtained from averaging three different repetitions with standard deviation as error bars.

2.5. Coatings preparation and application

The appropriate quantity of xanthan gum (0.2, 0.4, or 0.8 wt%) was added to the aqueous PLA dispersions as a thickener. Acid red 87 (0.01 wt%) was also added as a coloring agent in some formulations to visually estimate the coating uniformity. This mixture was then gently stirred magnetically (concentration 0.2 and 0.4 wt%) or mechanically (concentration 0.8 wt%) overnight.

Coatings on paper were obtained using close wound wire bar hand coaters with nominal wet film deposit thicknesses of 4 or 15 μm. The paper sheet was set up on a film coater pre-heated at 60 °C (TMAX Battery Equipment, Xiamen, China) and left there for at least 30 min after coating for drying.

2.6. Characterization of coated paper

Water absorptiveness of coated paper was measured by a 60-s Cobb test (Cobb60). The procedure was adapted from the Tappi T441 method using lab equipment. A 25 cm^2 testing sample of coated paper was laid, coated side up, on an impermeable surface, and a glass cylinder with 10.8 cm^2 of internal surface area was tightly clamped on this surface. 10.8 mL of ultrapure water was added within the cylinder and left there for 60 s. The coated surface was covered with a sheet of blotting paper and dried using a wooden roller. The sample was then immediately weighed on an analytic balance (0.1 mg precision). The Cobb60 (g/m^2) value was obtained by:

$$\text{Cobb60} = \frac{m_w - m_d}{A} \tag{1}$$

where m_w and m_d are the wet and dry weight, respectively, and A is the sample area equal to 0.00108 m^2. Tests were carried out in triplicate, and the standard deviation of the data was used as the uncertainty value.

Scanning electron microscopy (SEM) analyses were accomplished with a Zeiss EVO 40 microscopy (Carl Zeiss Microscopy Ltd., Cambridge, UK) equipped with a LaB_6 source. Samples in the form of coated paper or film were gold sputtered (15 nm coating thickness) before observation with a Quorum Q150R sputter coater (Quorum Technologies, Laughton, UK).

Paper sheet thickness was measured using a digital micrometer with 1 μm accuracy, by taking the average measurement of 4 points. Standard deviation was used as the uncertainty value for coated and uncoated paper thickness. Coating layer thickness was measured by SEM by selecting 4 representative points within a cross-section view of coated paper where the dividing line between PLA and cellulose fiber was clearly visible, measuring for each point the distance to the coating surface and taking the average distance as coating thickness. Standard deviation was used as the uncertainty value.

Cross-cut adhesion testing of prepared coatings was carried out as per ASTM D-3359 using an engraving tool and adhesive tape. The blade was run on the coated films in such a way that it should form a grille (1.5 cm × 1.5 cm) on the film. Then, adhesion tape was applied and pressed up to complete the adhesion on the surface of the coating, which was pulled off rapidly at an angle of 180° after 60 s. The sample portion that adhered to the tape was then observed to determine the degree of adhesion.

Water vapor transmission rate (WVTR) was measured using the desiccant method according to the ASTM E96 standard. 20 g of anhydrous calcium chloride was placed in an aluminum cup closed with a test sample. The coated side of the sample was faced out, and the bottom edges were sealed onto the cup with vinyl glue. Molten wax was poured onto the edge top so that 0.00385 m^2 surface area (A) was exposed to air. The samples were incubated at 22 ± 2 °C and 51 ± 3 % relative humidity (by saturated $Mg(NO_3)_2{\cdot}6\ H_2O$ solution), and their weight variation (0.1 mg precision) was monitored at time intervals that allowed for at least 20 mg of weight change. The analysis was over when at least 6 experimental points taken over at least 2 different days resulted in an R^2 value ≥0.998 by a linear fit. WVTR was calculated by the following equation:

$$WVTR = \frac{r}{A}\ g \Big/ (\text{days} \bullet m^2) \tag{2}$$

where r is the slope of the linear plot (in g/day) and A is the exposed surface area (in m^2). Water vapor permeability (WVP) was calculated from WVTR by the following equation:

$$WVP = \frac{WVTR \bullet L}{P} g \Big/ (\text{days} \bullet \text{Pa} \bullet \text{m}) \tag{3}$$

where L is the thickness of the sample (in m) and P is the water vapor pressure differential (in Pa) between the two sides of the sample (at 22 °C and 51 % RH, $P = 1348$ Pa). Tests were carried out in duplicate, and the standard deviation between samples was used as the uncertainty value.

Surface energy measurements were conducted in accordance with ASTM D2578 using Dyne Test inks (Ferrarini e Benelli, Romanengo (CR), Italy). The reported surface energy corresponds to the ink that separated into droplets approximately 2 s after application on the surface or the interval between a fully wetting and a fully non-wetting ink when no ink exhibited such a property.

Repulpability testing involved accurately weighing around 0.4 g of 2.5 × 2.5 cm square samples, soaking them in water at a concentration of 5 g/L at approximately 20–25 °C for 72 h, and stirring the samples magnetically at 450 rpm at 40 °C. In one approach, the sample was stirred until no individual fragment was visible to the naked eye, and the time was recorded. This was confirmed by ensuring that in each case, no sample remained on a 5 mm sieve. In the other approach, the sample was stirred for 2 h and then passed through the sieve. The elements remaining on the sieve were considered rejects, and their weight was measured after drying (at 60 °C overnight and 2 h at 100 °C). This weight was compared to the dry weight of the original sample to determine the reject rate.

3. Results and discussion

3.1. Synthesis of PEG-PLA-PEG triblock copolymers

mPEG-PLA-mPEG triblock copolymers (ELE) were synthesized using the one-pot, two-step diisocyanate coupling technique initially reported by Jeong and colleagues (Scheme 1) [39]. Methoxy-PEG (mPEG) served as the initiator for lactide polymerization, and the resulting ω-hydroxyl diblock copolymer was subsequently coupled with a diisocyanate to achieve the triblock structure. Our goal was to achieve a Hydrophilic-Lipophilic Balance (HLB) value similar to the one reported for the commercial Synperonic PE F/68 (SYN) surfactant utilized in our previous research [26]. Assuming a comparable hydrophobicity between PLA and PPG repeating units, we adjusted the amount of lactide in the feed to attain similar mass ratios between blocks as those reported for SYN (82 ± 2 % ethylene oxide content) [40]. Commercial mPEGs with nominal average molecular weights ($\overline{M_n}$) of 2 and 5 kDa were evaluated. However, when using the higher molecular weight mPEG, the resulting triblock copolymer exhibited insolubility in water at the desired concentrations of 1–3 % wt/v. We speculate that this outcome stemmed from the increased crystallization properties of the PLA block (consisting of 18 repeating units), leading to an excessive amount of PLA crystalline phase unable to arrange adequately in a surfactant-like manner in water. Consequently, the higher molecular weight mPEG was discarded, and

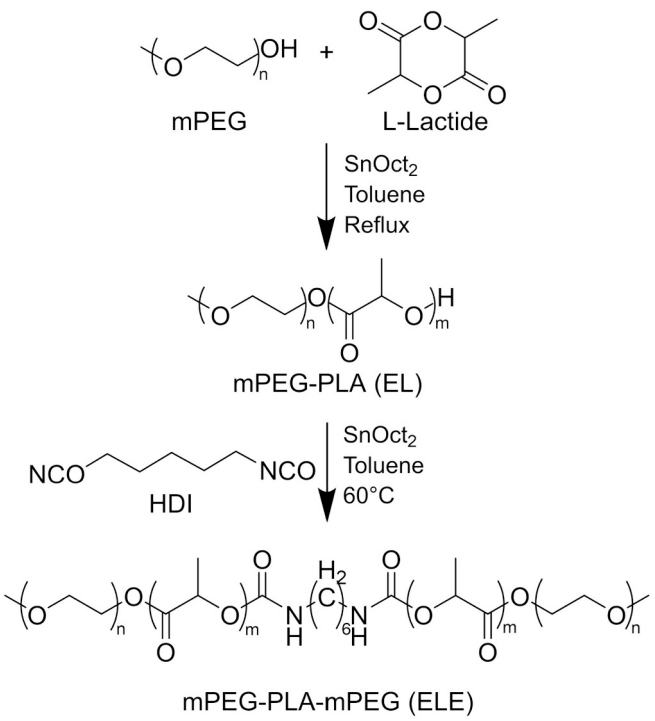

Scheme 1. Reaction for the synthesis of ELE copolymer surfactants.

only mPEG with an $\overline{M_n}$ of 2 kDa was employed. The resulting triblock copolymer featured a 2.8/1 M ratio of L-lactide to mPEG (Scheme 1).

The obtained ELE triblock copolymers exhibit a single peak in GPC-SEC analysis with an average molecular weight ($\overline{M_n}$) of 9.2 kDa, approximately double that of the EL diblock precursor (4.3 kDa), and a similar dispersity index of 1.06 (Fig. 1). The presence of a peak at 3.14 ppm in the ^{1}H NMR spectrum of ELE, attributed to the urethane-adjacent CH_2 by NMR analysis (Fig. 2, full spectrum in Fig. S1), confirms the coupling mechanism shown in Scheme 1. The number of repeating units of lactic acid in the EL precursor was approximately 4.7 when calculated

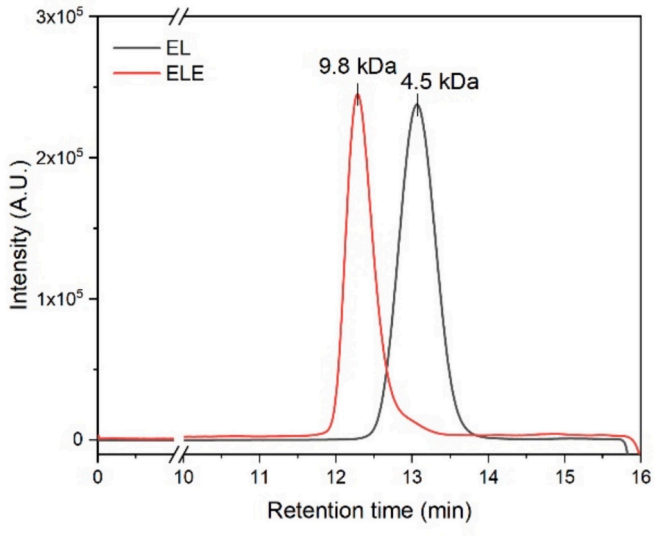

Fig. 1. Comparison of GPC-SEC chromatograms of the triblock ELE (red) and the diblock EL (black) copolymers. Signals from the RI detector are arbitrarily normalized to the same height. Peak molecular weight values are shown. (For interpretation of the references to color in this figure legend, the reader is referred to the web version of this article.)

by comparing the signal of the esterified terminal mPEG methylene (4.2–4.4 ppm) and the signal of repeating unit methines (4.9–5.3 ppm). This value is in reasonable agreement with the feed ratio (2.8/1 L-lactide to mPEG) once the actual lactide conversion is taken into account (approximately 90 %). The hydrophobic component, including both the PLA segment and the HDI coupling agent, thus accounted for around 17 wt% in the ELE triblock copolymer, very similar to the target range aimed for, analogous to that of SYN (16–20 %), although the molecular weight of ELE is lower (5.2 vs 9 kDa). The HLB is also similar, with the same Davies HLB value of 29, if the lactate repeating unit can be assumed to have similar hydrophobicity to the propylene oxide one or at 17 vs 16 if HLB is calculated via the simplified Griffin method [41].

3.2. Preparation and characterization of PLA dispersions

The preparation of waterborne PLA dispersions followed an oil-in-water method similar to our previous research [26]. Amorphous PLA was dissolved in ethyl acetate as the organic solvent. The two phases were homogenized using ultrasonication, and the organic solvent was then removed by evaporation at atmospheric pressure and room temperature.

A range of formulations was prepared using the ELE copolymer as the surfactant, either alone or in combination with SDS. The PLA concentration in the organic phase remained constant at 11 wt%, while the concentration of surfactants varied (Table 1). Samples were denoted as ELEx-SDSy, where x represented the concentration of the ELE surfactant (% wt/v), and y represented the concentration of SDS multiplied by 100 in the aqueous phase.

In the initial formulations, we tested ELE as the sole additive, at concentrations ranging from 1.8 % to 3.0 % (Table 1). The result was a homogeneous milky emulsion, stable in the immediate period following preparation. The solid content of these dispersions ranged from 13 % to 17 %, while particle size, as determined by DLS analysis, was approximately 600 nm for formulations using 2 % or less ELE as a surfactant, decreasing with increasing surfactant quantity to 512 nm for ELE2.4 and 380 nm for ELE3.0. The particle size distribution was multimodal in all cases, with polydispersity decreasing with size (Table S1). However, the long-term stability of these dispersions was limited. ELE1.8 and ELE2.0 showed the formation of evident precipitates within a week of preparation, indicating phase separation of part of the solid from the dispersion and sedimentation due to the density of PLA being greater than water. Surfactant concentrations higher than 2 % resulted in more stable dispersions, consistent with the reduced particle size. However, dispersions still displayed polymer precipitation after 1 and 2.5 months for ELE2.4 and ELE3.0, respectively. After 6 months, the solid content of ELE3.0 was 67 % of the original, indicating that 33 % of the solid had precipitated. While a dispersion stable over the long term (>6 months) could potentially be achieved by further increasing the surfactant content, we opted not to pursue this option due to the associated high hydrophilic surfactant content (above 20 wt%).

Instead, we opted to include a quantity of sodium dodecyl sulfate (SDS) as an anionic co-surfactant alongside ELE. We had previously observed that SDS with starch could stabilize waterborne PLA dispersions, but these dispersions were unable to film satisfactorily due to immiscibility with PLA [26]. Our goal was to add a small enough quantity of SDS to stabilize the dispersion without compromising the properties of films and coatings that could be obtained from them. Thus, we tested SDS concentrations ranging from 0.05 % to 2 % while keeping the ELE concentration fixed at 3 %, and ELE concentrations from 1 % to 3 % while keeping SDS fixed at 0.05 % (Table 1). In fact, SDS had a successful stabilizing effect even at just 0.05 % concentration. For example, ELE1.0-SDS5 remained stable for two months before precipitate formation, while ELE2.0, which contained double the quantity of neutral surfactant and no SDS, was stable for only a few days.

A reduction in particle size likely played a major role in improving dispersion stability. Fig. 3a shows particle diameter as a function of SDS

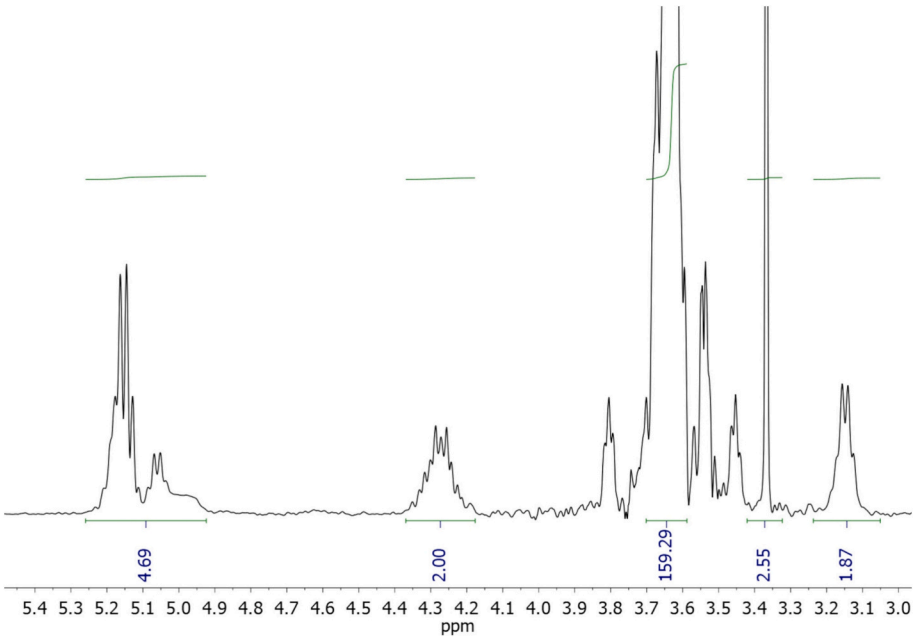

Fig. 2. Relevant portion of the ^{1}H NMR spectrum of the ELE surfactant in $CDCl_3$.

Table 1
Properties of aqueous dispersions of PLA using ELE and SDS as surfactants. All samples were prepared using 34 mL of organic phase containing 11 wt/v% PLA and 26 mL of aqueous phase.

Dispersion	ELE (wt%)[a]	SDS (wt%)[a]	D[b] (nm)	Solid content (wt%)	SC-6[c] (%)	Filmability at 60 °C	MFFT (°C)	ξ[d] (mV)
ELE1.8	1.8	0	590	13	–	–	–	–
ELE2.0	2	0	670	14	–	–	–	–
ELE2.4	2.4	0	510 ± 40[e]	17 ± 3[e]	–	Good	–	–
ELE3.0	3.0	0	380 ± 40[e]	16 ± 1[e]	67	Good	38	−48.7 ± 0.4 (−36 ± 1)
ELE3.0-SDS5	3.0	0.05	290 ± 10[e]	16 ± 1[e]	83	Good	46	−62 ± 3 (−34 ± 1)
ELE2.4-SDS5	2.4	0.05	340 ± 20[e]	18 ± 2[e]	72	Good	41	−65 ± 3 (−38 ± 2)
ELE1.5-SDS5	1.5	0.05	370	17	67	Good	49	−72 ± 2 (−48 ± 2)
ELE1.0-SDS5	1.0	0.05	450	15	62	Good	47	−45.8 ± 0.2
ELE3.0-SDS10	3.0	0.1	260	15	93	Good	44	−67 ± 1 (−50 ± 1)
ELE3.0-SDS40	3.0	0.4	220	20	95	Opaque	46	−61 ± 2 (−31 ± 1)
ELE3.0-SDS200	3.0	2	190	18	94	Cracked	nd	−46 ± 1 (−36 ± 2)

[a] Concentration in water phase.
[b] D = hydrodynamic diameter as Z-average value by DLS analysis.
[c] Solid content after 6 months as % of the original value.
[d] Value after 6 months in brackets.
[e] Average value across 3 separate preparation.

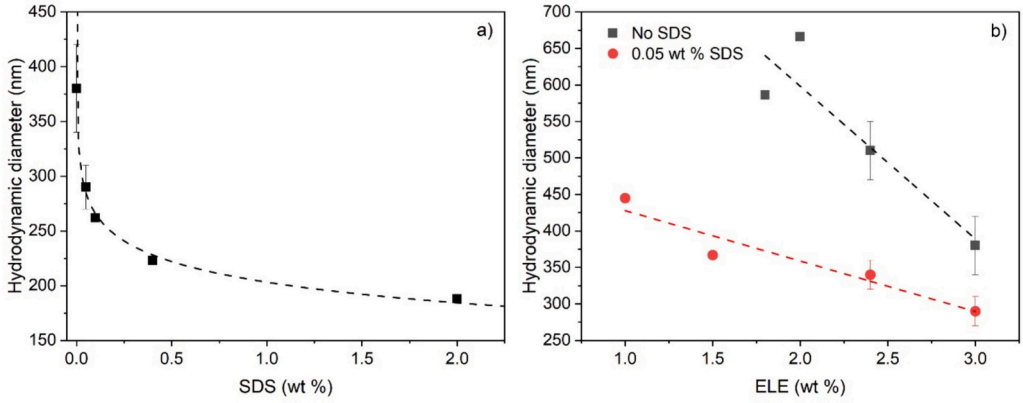

Fig. 3. Hydrodynamic diameter (as measured by Z-average) of the particles in waterborne PLA dispersions versus: a) SDS content when ELE content was fixed at 3 %, b) ELE content when SDS was absent (black) or fixed at 0.05 % (red). Possible logarithmic (a) and linear (b) fit curves are also shown. (For interpretation of the references to color in this figure legend, the reader is referred to the web version of this article.)

content when the ELE concentration was fixed at 3 %. Indeed, the addition of SDS in the smallest amount (0.05 %) was sufficient to reduce the particle diameter from 380 to 290 nm, while further addition had a lesser but still relevant effect, with the minimum diameter of 188 nm being reached at the highest SDS concentration, 2 %. We identified a logarithmic ($R^2 = 0.98$) dependence of the diameter on SDS concentration, consistent with observations in literature for polymer latexes obtained by emulsion polymerizations [42–44]. Surfactant molecules arrange themselves at the interface between the organic and aqueous phases, leading to smaller droplets of the organic phase dispersed in water as the quantity of surfactant increases. However, there is a maximum surface area stabilization beyond which further increases in surfactant concentration do not affect particle size [43], resulting in the observed logarithmic trend in Fig. 3a. Increased ELE concentration also reduced particle size, as shown in Fig. 3b. When the SDS content was fixed at 0.05 %, the dependence of particle size on ELE content was nearly linear ($R^2 = 0.92$), with higher ELE content resulting in smaller particle size. A linear dependence was also possible when no SDS was used, but the correlation was less clear in this case, likely due to the multimodal and polydisperse nature of large particles, making such a trend harder to detect for low surfactant content. DLS polydispersity index (PDI) generally increased along with particle size (see Table S1). When the z-average diameter was above 350 nm, PDI was >0.25, and the size distribution by intensity analysis was multimodal. Conversely, when the diameter was below 350 nm, PDI was <0.25, and the size distribution was monomodal, with a peak close to the z-average value (see Table S1).

The particle size distribution was also more reproducible when SDS was added: ELE2.4-SDS5 and ELE3.0-SDS5 formulations were replicated three times each, and the relative standard deviation of particle diameter across these preparations was small in both cases (5 % and 7 %, respectively). In contrast, the ELE3.0 formulation without SDS had a relative standard deviation (SD) of 11 % across three replications.

The qualitative observation of dispersion stability proved difficult when extended over a period of several months, as the buildup of precipitate can be very gradual. Thus, ultimately, stability over time was evaluated quantitatively by measuring solid content after 6 months and comparing it to that of freshly prepared dispersions (Table 1). Fig. 4 shows the dependence of dispersion stability on the content of the two surfactants. The trends observed for stability were quite similar to the ones previously outlined for particle size, supporting the correlation between these two properties. Addition of SDS, even in small quantities, had a dramatic effect on stability, with the residual solid content increasing from 67 % to 93 % between ELE3.0 and ELE3.0-SDS10. On the other hand, the addition of SDS beyond 0.1 % did not cause a further increase in stability, as a decrease of approximately 5 % in solid was noticed even when high quantities of SDS (up to 2 %) were added. When SDS content was fixed at 0.05 % and ELE content was varied from 1 to 3 %, we once again noticed an almost linear ($R^2 = 0.94$) increase in dispersion stability, with a trend similar to the one observed for particle size (Fig. 4).

Apart from the stability of PLA dispersions, the hydrolytic stability of the polymer itself in the aqueous dispersion is also a potential concern, as the backbone ester groups are vulnerable to hydrolysis, causing a reduction in molecular weight and potentially negative effects on the properties of the final polymer coating [45]. We monitored the molecular weight of ELE3.0-SDS5 for up to 10 months during storage at 4 °C. GPC analysis of the dispersions shows two main peaks, the first due to the high molecular weight PLA (HMW) and a second at lower molecular weight due to both the ELE surfactant and hydrolyzed shorter PLA chains (LMW) (Fig. 5a). In order to follow the degradation of PLA, the area decrease of the HMW contribution above 28 kDa was monitored. Indeed, as the degradation progresses, the polymer molecular weight decreases, and the chains are eluted at higher retention times. As a result, the HMW area (A_{HMW}) decreases, and the LMW one (A_{LMW}) increases. The reduction over time of the normalized HMW areas was thus

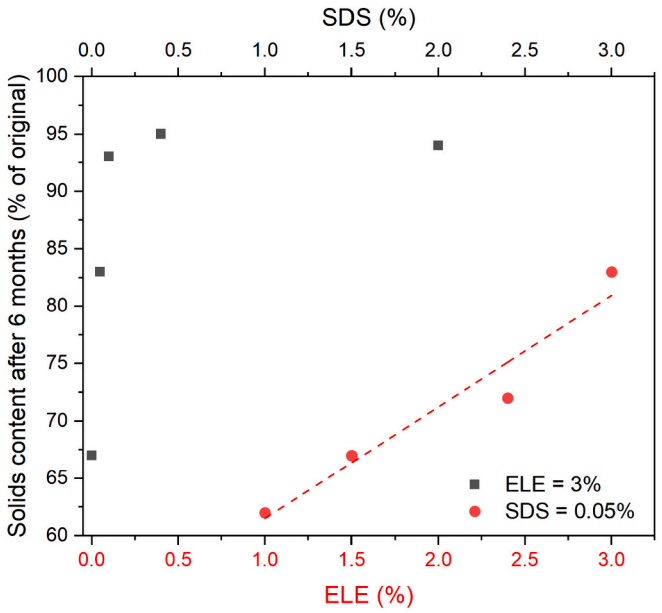

Fig. 4. Stability of prepared PLA waterborne dispersions was evaluated by the percentage ratio of solid content after 6 months to the original solid value versus the surfactant content. Values shown in black are for an ELE content fixed at 3 % and SDS content varying in the 0–2 % range, while values shown in red have an SDS content fixed at 0.05 % and an ELE content varying in the 1–3 % range. A possible linear fit is also shown for the latter. (For interpretation of the references to color in this figure legend, the reader is referred to the web version of this article.)

assumed as the hydrolysis index (HI).

$$HI = \frac{A_{HMW,t}/(A_{HMW,t} + A_{LMW,t})}{A_{HMW,0}/(A_{HMW,0} + A_{LMW,0})} \quad (4)$$

where $A_{HMW,0}$ and $A_{LMW,0}$ are the areas of the GPC peaks above and below 28 kDa, respectively, in the chromatogram of a freshly prepared dispersion. $A_{HMW,t}$ and $A_{LMW,t}$ are the same areas in the chromatogram of a dispersion stored for time t. As this value is defined, it is equal to 1 at the beginning of storage and tends to 0 over time as the quantity of HMW polymer decreases; HI = 0 being a completely degraded PLA with no HMW fraction present.

The evolution of HI over time, compared to $\bar{M}_n$ calculated within the HMW section after the same storage time, is shown in Fig. 5b. As the two values change in similar ways, this supports the assumption that the molecular weight lost within the HMW area is transferred to the LMW area through PLA hydrolysis. PLA hydrolysis develops linearly and slowly for the first 7.5 months with the loss of approximately 2 % of the HMW mass for each month in storage. The hydrolysis rate then strongly increases after this period with a loss of 18 % of HMW mass within the next 2.5 months. This acceleration is attributed to the autocatalytic effect of carboxylic acid groups that form upon hydrolysis [36].

Storage for up to a 7-month period of the dispersions should limit polymer degradation within parameters acceptable for most applications, but storage over a longer period is unadvisable due to the acceleration of hydrolysis. A typical validity period of many commercial polymer emulsions is 6 months; therefore, the observed stability is compatible with actual industrial practices.

Observing the SEC chromatograms, we also found that apart from the ELE peak, an additional well-defined peak was present at 4.2 kDa after 4 months of storage (Fig. 5a). The most likely attribution for this peak is the splitting of the ELE surfactants in two portions; indeed, it may be noticed that its molecular weight is approximately half the one of ELE, and very similar to the one of the EL diblock prepolymer obtained before

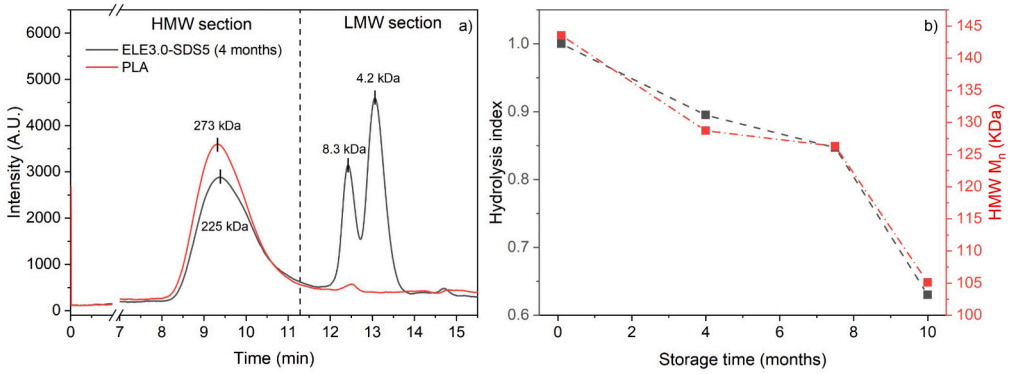

Fig. 5. a) GPC-SEC chromatograms (RI detector, chloroform eluent) of commercial PLA 4060D (red) and dried ELE3.0-SDS5 waterborne PLA dispersion after 4 months of storage at 4 °C (black). Peak molecular weight values shown; b) hydrolysis index and $\overline{M_n}$ in the HMW-section as a function of storage time at 4 °C. (For interpretation of the references to color in this figure legend, the reader is referred to the web version of this article.)

the isocyanate-promoted coupling (Fig. 1). The ester groups of ELE are more likely to have been hydrolyzed as compared to the more stable urethane bonds. The surfactant is in more intimate contact with the aqueous phase compared with the PLA itself, and this should expose the short PLA section of ELE to hydrolysis more compared to the homopolymer chains. The hydrolysis of both PLA and ELE results in the formation of carboxylic groups, which was confirmed by pH measurements. Freshly prepared dispersions have a pH around 4, the acidity being probably attributable to carboxyl end groups of PLA; assuming each PLA chain contains a carboxyl group, the concentration of these groups would be around 1 mM, resulting in a pH of 3.5 assuming the pK_A of lactic acid and complete availability for proton exchange. After 6 months of storage, the pH of the dispersions was around 3, thus being increased by surfactant and polymer hydrolysis.

Measurements of the Z-potential (ξ) of PLA dispersions may also help to better elucidate their structures and understand their stability over time. Freshly prepared dispersions had negative z-potential (ξ) in the −46 to −72 mV range, (Table 1), with most of the samples having ξ values below −60 mV. This range of values is typical of stable colloids [46]. No clear relationship could be found between ξ values and the type and quantity of additives. For comparison, Abdenour and colleagues [29] also obtained negatively charged stable PLA dispersions with a ξ value of −39 mV using commercial non-ionic surfactants. While they attributed this property to the capability of non-ionic surfactants to selectively absorb OH^- ions from water, we consider the negatively charged character of the particles to be primarily attributable to the carboxyl end-groups of the PLA chains, which may be more or less exposed on the particle surface depending on surfactant and dispersion preparation. Interestingly, testing after 6 months of storage showed a significant increase in ξ for all samples, ranging from a 20 to a 50 % decrease in absolute value. This is most likely tied to the decrease in pH over time as previously described, which would in general cause an increase in ξ values, as well as to gradual particle aggregation. The decrease in absolute value of ξ to a range typical of moderate rather than good colloid stability may be a cause of the limitation in long-term stability of dispersions previously described. However, it cannot fully explain it, as samples with high stability with regards to suspended solid (95 % solid retained after 6 months) still had similar ξ values to the ones with lower stability.

3.3. Properties of films obtained from waterborne PLA dispersions

The minimum film forming temperature (MFFT) of a waterborne formulation is one of its most important properties; above this temperature the coating is continuous due to particle coalescence, while below it a heavily cracked and discontinuous surface is formed, and particles generally remain separated from each other. MFFT is closely related to the glass transition temperature (T_g) of the waterborne polymer, but this relationship is not a simple one as, depending on the polymer/surfactant system and other additives; MFFT may have values either lower or greater than the T_g of the dried polymer. It is however generally accepted that plasticization of the waterborne polymer will lower MFFT along with T_g [47–49].

PLA waterborne formulations were in general capable of forming a semi-transparent (74–86 % transmittance at 600 nm) and continuous film when heated to 60 °C (Table 1, transmittance data reported in Table S2, sample film in Fig. S2), slightly above the glass transition temperature of pristine PLA (54 °C). The only exceptions happened when SDS was added in the largest concentrations: 0.4 % SDS led to an opaque but still continuous film, while the dispersion containing 2 % SDS was unable to satisfactorily form a film due to macroscopic effects of polymer-surfactant immiscibility that leads to a discontinuous surface. Films cast from ELE3.0-SDS5 at various temperatures were observed by SEM to better discern the influence of temperature on film formation (Fig. 6). Drying the dispersion at room temperature (23 °C) resulted in a heavily cracked and opaque surface. However, from SEM imagery we observed, not the single particles from the dispersion but still a heavily irregular and discontinuous surface (Fig. 6a). This suggests that some particle coalescence still happened at room temperature, creating local continuous domains (< 10 μm wide) but that only a subset of dispersed particles was able to fuse with its neighbors, resulting in the overall discontinuity. Increasing the casting temperature, we observed that the surface became composed by two different kinds of large (> 100 μm wide) domains (Fig. 6b–e), on the one hand some distinguished by a continuous homogenous surface, on the other hand by an irregular one, similar to that observed when dried at room temperature. The ratio of continuous film domains to the overall surface increased with temperature.

Macroscopically we observed that at 47 °C the cast dispersion was mostly transparent, while at 45 °C it was opaque. This corresponded to a marked increase in the film to surface ratio observed by SEM. At 60 °C the entire surface of the dried dispersion was composed by a continuous film, with no particle or particle separation visible (Fig. 6f). For some selected formulations (see Table 1), we thus carried out qualitative determination of film forming by drying dispersions at 1 °C intervals to find the temperature at which the surface became transparent, defined as MFFT (Fig. S3).

This qualitative observation is indeed the most common technique to determine MFFT [50]. The obtained values (Table 1) ranged from 38 to 49 °C, below the T_g of pristine PLA (54 °C) but above room temperature. ELE3.0 had a MFFT of 38 °C, which increased to 46 °C when 0.05 % SDS was added, but no further increase in MFFT was noticed as SDS content was further increased. This seems to indicate that the presence of the anionic surfactant causes an increase in MFFT, but this is not then

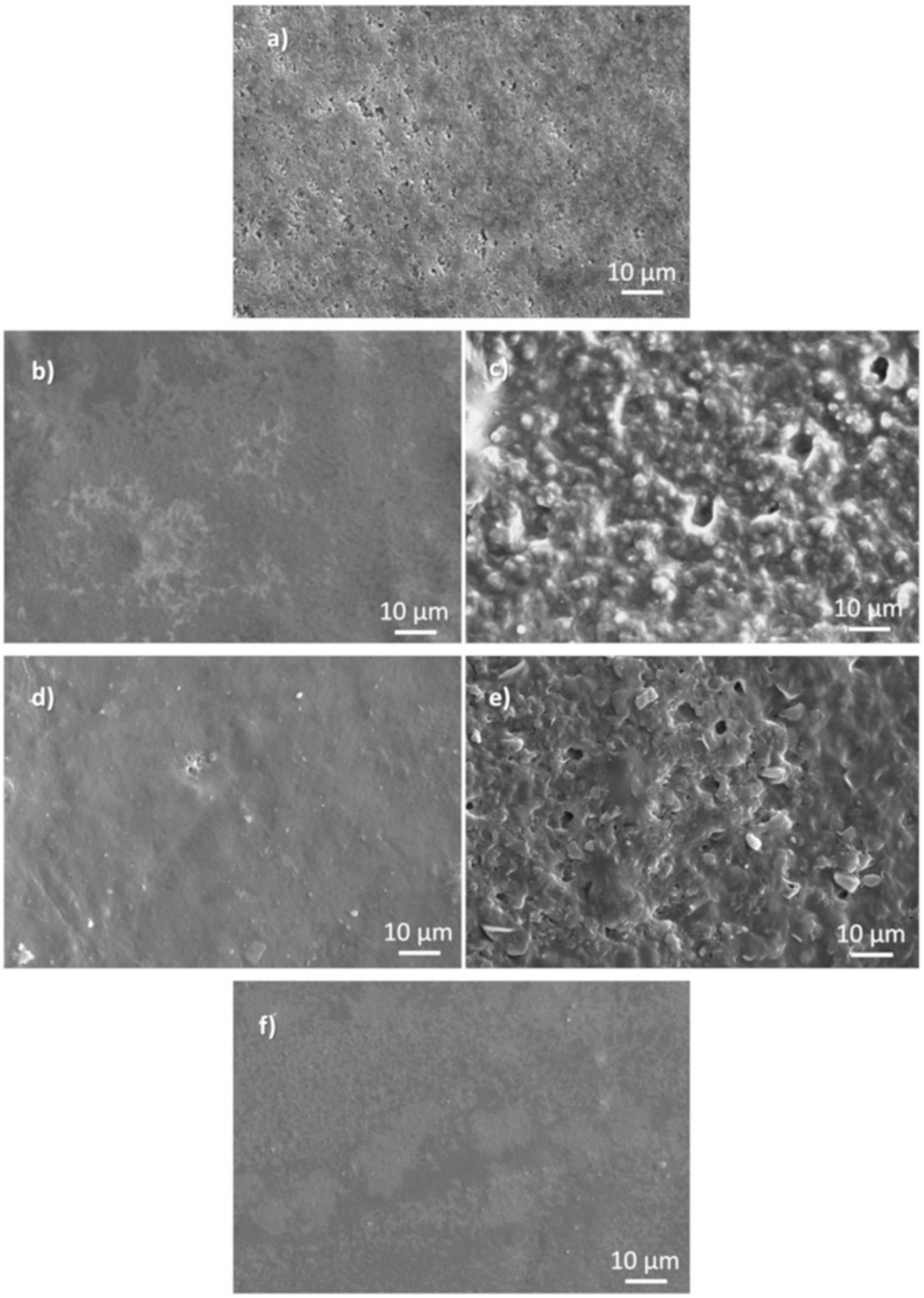

Fig. 6. SEM images (3000× magnification) of PLA films cast from ELE3.0-SDS5 at: 23 °C (a), 45 °C (b and c), 47 °C (d and e), 60 °C (f). Side-by-side images display different regions of the same film displaying different morphology, continuous on the left and discontinuous on the right.

dependent on SDS concentration within the tested range.

The attempt to analyze the T_gs of dried polymer films and relate this to MFFT was complicated by the presence of surfactant melting peaks within the DSC thermograms (Fig. S4). The existence of non-miscible surfactant domains in films and coatings obtained from waterborne polymers is rather common and may cause diminished adhesion and water resistance properties as such hydrophilic domains migrate to the film surface [51–53]. In our case, we identified the frequent appearance of a peak around 50 °C in DSC thermograms with the presence within the sample of crystallized ELE domains, as the melting peak of the pure block copolymer was observed at 51 °C (Fig. S4). The presence of this peak influenced the nearby T_g transition by shifting the inflection point of the transition, thus making apparent T_g values higher (sample thermograms with and without this peak within a single film are shown in Fig. S4). It also made these values unreliable, as different regions of the films displayed different apparent T_g values with variations reaching over 10 °C within the same film, thus making comparison between formulations hard to do. It is however worth noting that even the apparent T_g values (reported in Table S3), which ranged from 20 to 40 °C, were always lower than the one of pristine PLA, meaning that the ELE surfactant was effective as plasticizer of the polymer, and they were also lower than the observed MFFT value of the corresponding formulation. In particular, the addition of 3 % ELE and SDS below 0.1 %, which corresponds to a 20 % surfactant/polymer weight ratio, resulted

in a T_g of 23–27 °C when the surfactant melting peak did not interfere with the measurement. This is in accordance with our previous research, which showed rather similar apparent T_g values when a PEG-PPG-PEG copolymer was used as surfactants, while the T_g of the SDS-based formulation was unchanged from pristine PLA [26]. PEG oligomers alone are good plasticizers for PLA. A 10 wt% PEG content has been shown to reduce the T_g of PLA to 30 °C and the same is also true for PLA-PEG-PLA triblock copolymers, which have been reported in literature and have been shown to have a similar effect when added in a 20 wt% ratio to the polymer [34].

3.4. High-solid PLA dispersions

The solid content of the dispersions obtained directly by the oil-in-water technique was lower than 20 wt%. Attempts to increase this value by either increasing the ratio of organic to aqueous phase during preparation or the concentration of PLA in the organic phase ran into physical limitations or issues of excessive solvent use [26]. Thus, the most accessible way to increase solid content is to remove water from the prepared dispersions until the desired content is reached. Indeed, water evaporation already occurs to a limited degree concurrently with that of the organic solvent during the initial dispersion preparation, leading to solid content slightly higher compared to the theoretical value. This process can be accelerated by removing water under moderate reduced pressure.

The quantity of surfactant used proved to be decisive in determining how far the concentration process may be taken forward until macroscopic particle coalescence occurs. ELE1.5-SDS5 became unstable when the dispersion volume was reduced to 60 % of the original (~ 25 % solid), while ELE3.0-SDS5 only became unstable at 33 % of the original volume (~ 50 % solid). When the solid content was fixed at 40 ± 5 wt%, the latter formulation was found to be dimensionally unchanged when analyzed by DLS (diameter was 290 ± 10 nm across 3 replicates, the same as the original value). It was also stable by visual inspection for at least a month, as no sedimentation or creaming occurred. Quantitatively, the solid content of a concentrated ELE3.0-SDS5 sample that was originally 40 wt% after 6 months was found to still be 33 wt%, which is 83 % of the original. Stability properties were thus only slightly worse than those of the unconcentrated corresponding sample. This formulation was then adopted as the model high-solid dispersion for coating studies.

3.5. Viscosity of PLA dispersions

Viscosity as a function of shear rate for ELE3.0-SDS5 PLA dispersions at low-solid (16.0 ± 3.0 wt%) (PLA15) and high-solid (40.0 ± 5.0 wt%) (PLA40) concentrations is shown in Fig. 7. At low shear rates, PLA40 exhibits a viscosity plateau value two orders of magnitude greater than that of PLA15, attributed to the higher particle density in the former sample, which acts as obstacles to flow. With increasing shear rate, both samples exhibit non-Newtonian shear thinning behavior well described by the Cross model (fitting of the various samples according to the Cross or power law models is described in the supporting information, Table S4). The viscosity trend of PLA15, within error bars, is in good agreement with previous measurements on a similar sample (15.0 ± 0.1 wt%) [27].

Waterborne dispersions of polymers typically require the addition of a thickening agent to be coated on paper, as the pristine viscosity is usually very low, allowing particles to permeate into the pores of the paper substrate rather than forming a layer on top of the fiber network. For this purpose, we selected xanthan gum (XG), a microbial polysaccharide widely used in various industries, including as a food additive. XG aqueous solutions exhibit pseudo-plastic behavior with high viscosity even at low concentrations and are stable to temperature and pH changes [54]. In our testing, we primarily focused on the high-solid formulation previously obtained by concentration (40 ± 5 wt%), while varying the XG concentration in the aqueous phase from 0.2 to 0.8 % (wt/v). For comparison purposes, we also tested PLA15 (16 ± 3 wt%) with 0.4 % of XG. This approach was chosen to minimize the thickener's impact on the coating. For a 40 wt% solid content, the addition of 0.2, 0.4, and 0.8 % of XG in the aqueous phase results in XG content in the dry film of 0.5, 1, and 2 wt%, respectively, while in the low-solid alternative, all these values are 2.5-fold larger.

The viscosity behavior of XG alone was also evaluated while varying XG concentration from 0.2 to 0.8 % in water (Fig. S5). At all concentrations, the solutions exhibited shear thinning behavior without an evident low shear rate plateau. Viscosity increased with concentration as expected, and the data were well fitted through a power law equation (Table S4).

Fig. 8 shows the comparison among the flow curves of the high-solid concentrated PLA sample (40.0 ± 5.0 wt%) with and without XG and the reference XG solution at three different weight concentrations of XG: 0.2, 0.4, and 0.8 %.

All curves exhibited shear thinning behavior and indicated that the addition of XG to the PLA dispersion hindered the formation of a Newtonian plateau at low shear rates. The viscosity of the samples increased by an order of magnitude compared to both the high-solid PLA without XG and to the XG solution. For comparison, in Fig. 7b, we report the viscosity of the low-solid formulation at 0.4 % XG concentration as an example. In this case, the addition of XG modified the shape of the curve as well. However, in contrast to the case of the high-solid sample, the viscosity of the low-solid one with 0.4 % XG appeared very similar to that of the XG reference solution, indicating that at low PLA concentration, XG is the main significant component that affects rheological

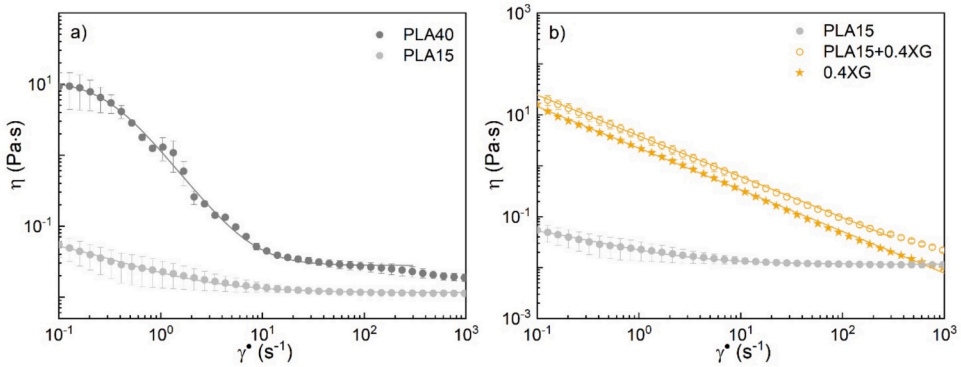

Fig. 7. a) Viscosity of ELE3.0-SDS5 as a function of shear rate for low-solid (PLA15) and high-solid (PLA40) samples. Lines represent fits through the Cross model. b) Viscosity as a function of shear rate for PLA15 with and without XG, and the reference XG solution at a concentration of 0.4 %. Lines represent fits through the power law and Cross models (fitting parameters in Table S4).

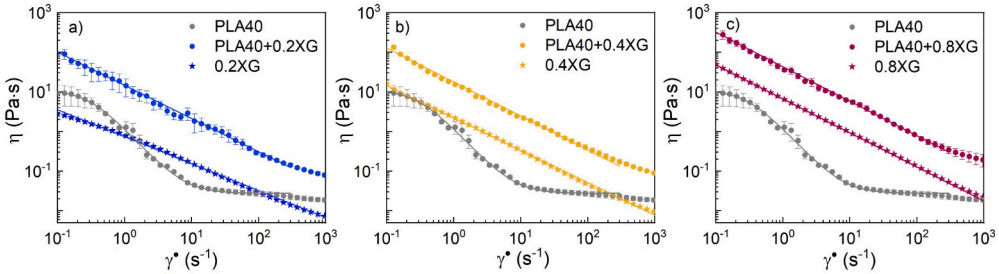

Fig. 8. Viscosity as a function of shear rate for the high-solid sample (PLA40) with and without XG, and the reference XG solution, at XG concentrations of (a) 0.2 %, (b) 0.4 %, and (c) 0.8 %. Lines represent fits through the power law and Cross models.

behavior, while at high solid-content both the PLA and the XG components have a contribution. This demonstrates that we are able to obtain the desired rheological behavior and thus optimize the coating formulation by both the addition of a small amount of XG and by changing the solid content in the waterborne PLA dispersion.

3.6. Application and properties of PLA paper coatings

The substrate used for testing was standard printing paper. This paper was coated using bars capable of applying two different nominal thicknesses of liquid layer, 4 and 15 μm (Table S5). The coating was applied at 60 °C to work above MFFT. We anticipated, based on previous literature on the subject [20,25,29], that more than one application of the coating would be necessary to obtain satisfactory surface coverage and thus properties. Therefore, for each formulation, a number of applications varying from 1 to 4 was tested (Table S5). We also aimed to limit coating weight due to recyclability issues of the final product.

SEM micrographs in Fig. 9 show surface views of paper sheets coated with successive applications of a 4 μm liquid film with PLA40 and 0.8 % XG. Upon observation, the surface of the sample with a single application (6 g/m^2 of coating weight, Fig. 9b) revealed that the pulp fibers making up the paper sheet (Fig. 9a) were not completely covered by the coating but were visible on the surface. Conversely, when the film was applied twice (10 g/m^2 of coating weight, Fig. 9c), the surface was completely covered by the coating, and the fibers were no longer visible. All other samples on which at least two layers of coating were applied, with any high-solid formulation, also displayed a continuous coated surface where the underlying cellulose fiber network was not visible.

Fig. 10 depicts cross-section images of coatings produced with the same formulation with an increasing number of applied 4 μm layers. In the first row, a single application (Fig. 10b) results in a smoother surface compared to pristine paper (Fig. 10a), but the coating is not distinctly visible as a separate element from the cellulose. However, with increasing applications of the same liquid film (Fig. 10c, d, and e corresponding to 10, 12, and 15 g/m^2 coating weight), a separate PLA coating layer becomes visible. These images illustrate its increasing thickness and the maintenance of its homogeneity, with no visible separation within it as successive layers are applied.

Further observations highlight the effect of different viscosities of the waterborne dispersion that was coated on the paper surface. Images f, g and h in Fig. 10 show cross-section views of paper sheets coated with PLA40 containing 0.4 % XG, respectively with 10, 15 and 21 g/m^2 coating weight. A PLA coating layer is still clearly visible and fully covers the paper surface, but it is harder to distinguish the separating line between this layer and the paper underneath. This suggests that a greater part of the dispersions enters paper pores rather than forming a surface layer. The effects of a further reduction in XG content to 0.2 % are shown in images i and j in Fig. 10 (respectively corresponding to 10 and 15 g/m^2 of coating weight). With 10 g/m^2 of coating weight, the PLA layer was not distinguishable as a separate element from the cellulose fibers, while at 15 g/m^2 the overlap between the cellulose fibers and the coating was even more evident than previous observation, with PLA being observed filling paper pores to a depth > 5 μm from the paper surface. Thus, a reduction in the viscosity (from 36 to 14 Pa•s at 1 s^{-1} shear rate, Table S4) of the applied waterborne dispersion results in its deeper penetration within the paper and the formation of a thicker intermediate layer composed by paper with pores filled by the coating.

Another observation is that the surfaces of coated paper samples made with 0.2 % XG were significantly more irregular than those made with a higher XG amount (Fig. 11). This could be attributed to the lower flattening ability of the formulation with low viscosity, which does not form a compact layer on top of the fiber network but rather covers the individual fibers.

The partial penetration of the polymeric coating within the fibers of the paper that we observed, promoted by the use of waterborne technology, should improve adhesion to the substrate compared to extrusion coating, especially in the case of thin film layers [55,56]. Indeed, we achieved good adhesion to the substrate with all tested formulations and under all application conditions: the PLA coating could not be removed by mechanical means. When a Scotch tape cross-cut peel test was attempted, there was either no detachment or the removal of a significant amount of paper fibers in the cross-cut area rather than the coating itself, indicating that the adhesion energy of the coating to the paper substrate was higher than the internal cohesion energy between the

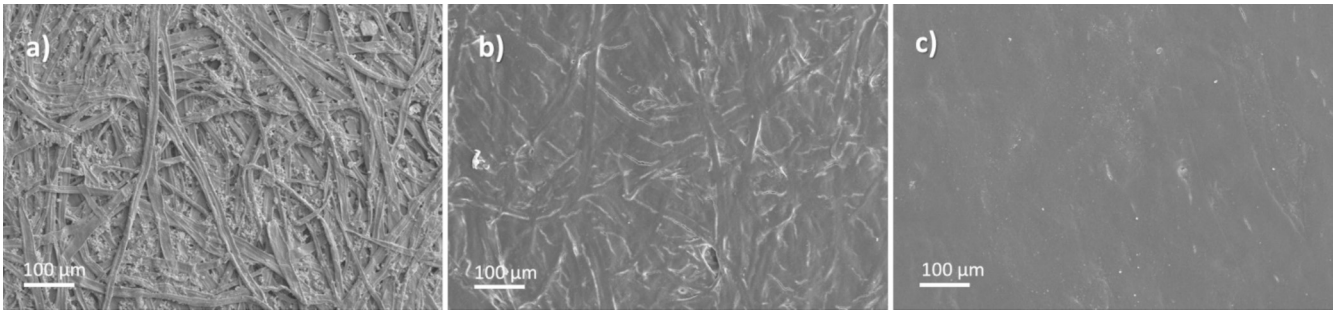

Fig. 9. SEM images (400× magnification) of: a) uncoated paper, b) paper coated with 1 application of 4 μm film of PLA40 with 0.8 % XG content, c) paper coated with 2 applications of 4 μm film of PLA40 with 0.8 % XG content.

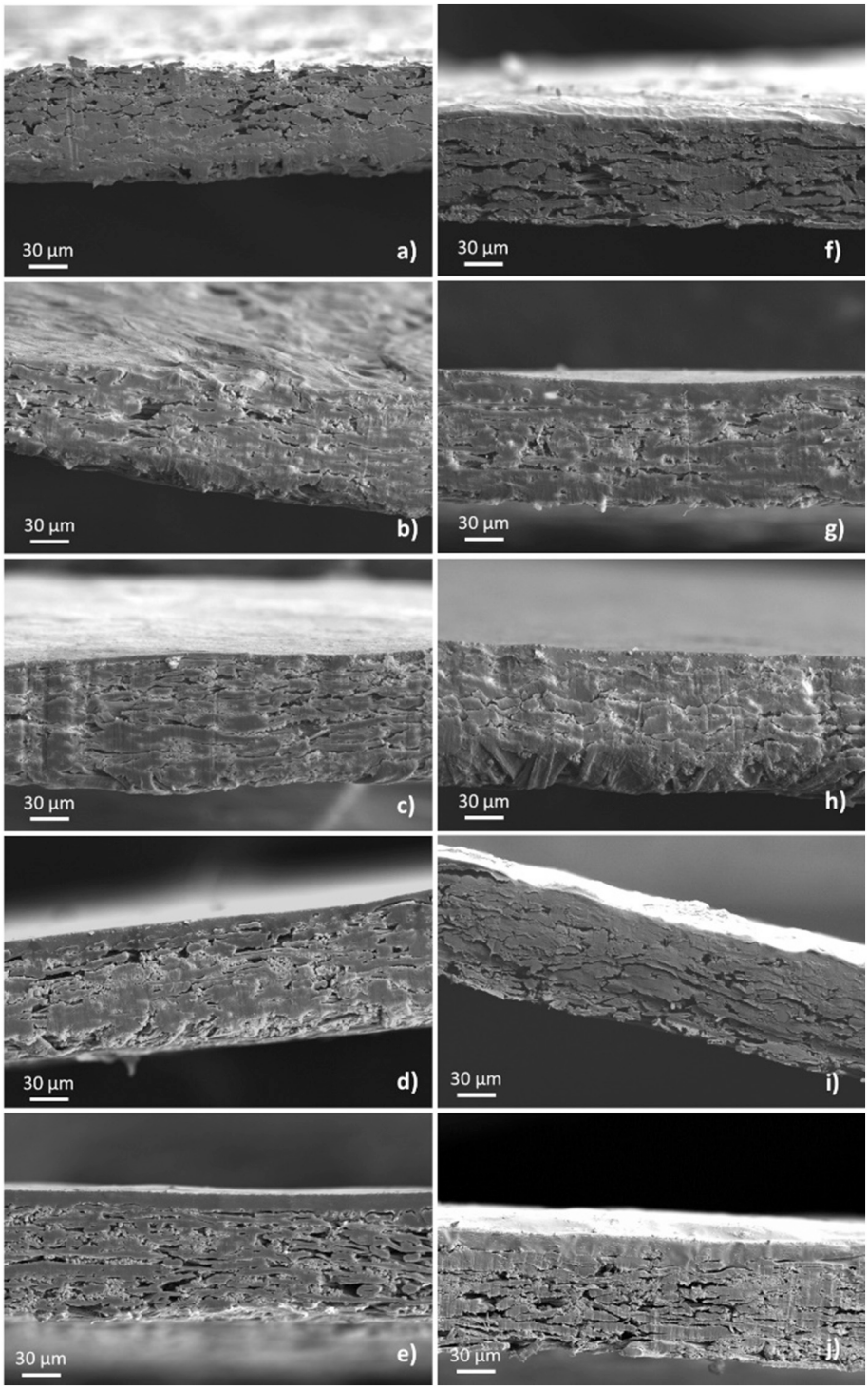

Fig. 10. SEM images (1000× magnification) of the cross-section of paper samples. In the first colum, uncoated paper (a) followed by paper coated with PLA40 with 0.8 % XG in an increasing number of 4 µm applications from 1 to 4 (b–e). The coating weight of these samples is, in order, 6, 10, 12 and 15 g/cm^2. In the second column, paper coated with PLA40 under different conditions (XG content, applications and coating weight): (f) 0.4 % XG, 2 × 4 µm, 10 g/m^2, (g) 0.4 % XG, 3 × 4 µm, 15 g/m^2, (h) 0.4 % XG, 3 × 15 µm, 21 g/m^2, (i) 0.2 % XG, 2 × 4 µm, 10 g/m^2, (j) 0.4 % XG, 4 × 4 µm, 18 g/m^2.

paper fibers [57,58].

The water resistance of paper coated under different conditions was studied using Cobb60 tests, and the results (Fig. 12, Table S5) showed that a single layer application was ineffective in conferring water resistance with any formulation tested. This result aligns with SEM observations that showed incomplete coverage in these cases. The coating resulting from the first application acted as a primer, which did not reduce water absorptiveness compared to pristine paper but rather smoothed out the surface to allow for more effective coating layers in subsequent applications. In Fig. 12a, we highlight the results obtained using only the high-solid formulation (PLA40) with multiple applications, divided into three groups depending on the XG content present. Coating weight increased, as expected, with both the number of applications and the thickness of the liquid layer deposited, ranging from 9 to 21 g/m^2. Water absorption across these tests was always reduced compared to that of pristine paper (100 ± 10 g/m^2) but varied strongly,

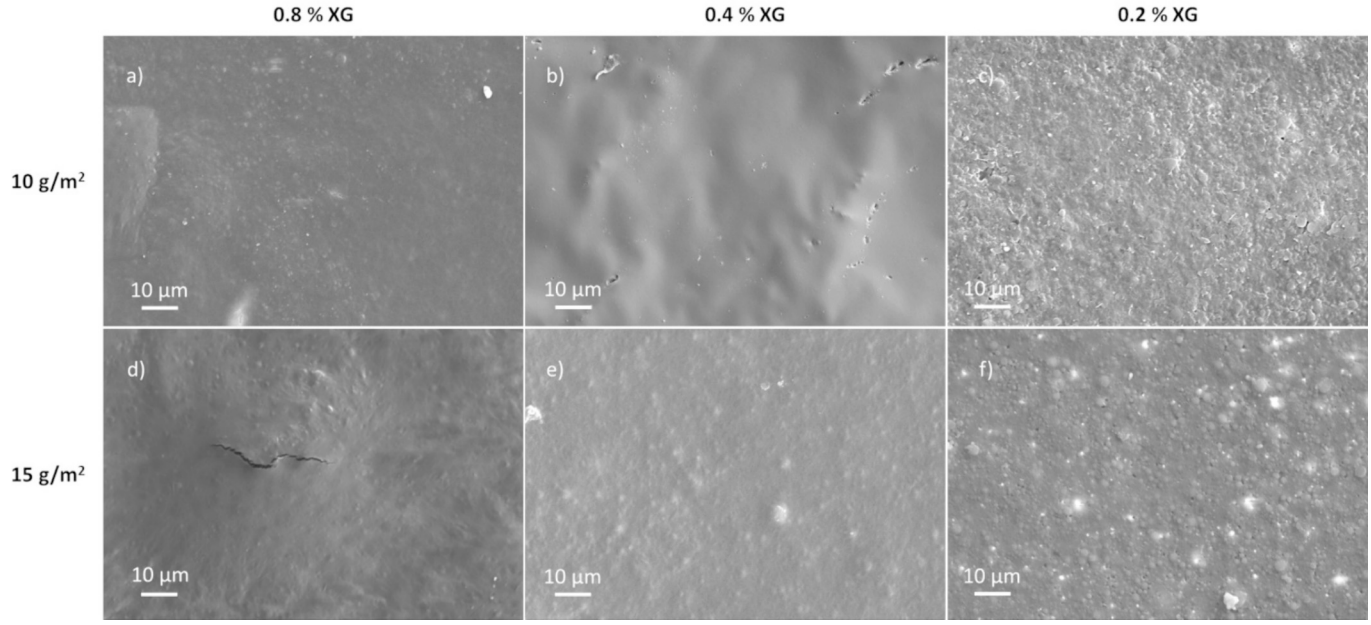

Fig. 11. SEM images (3000× magnification) of coated paper using PLA40 formulation with different contents of XG (0.2, 0.4 or 0.8 wt/v%) and at two different coating weights, 10 and 15 g/cm^2.

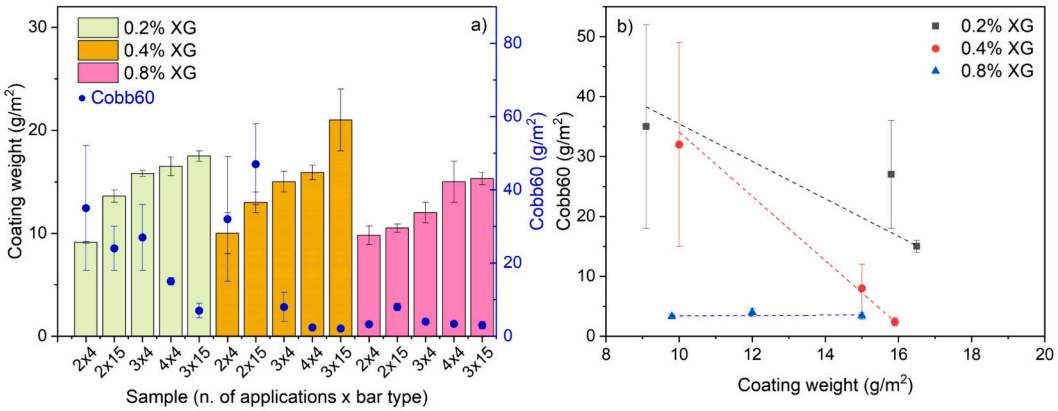

Fig. 12. a) Coating weight and Cobb60 index of PLA-coated paper obtained with PLA40 formulation (solid content 40 ± 5 %). Each column describes a coating obtained by multiple (2 to 4) applications of liquid film using a 4 or 15 µm bar. Different colors indicate different XG concentrations. b) Cobb60 index as a function of coating weight by 2 to 4 applications of liquid film using a 4 µm bar, linear fits are shown as dashed lines.

from 50 to 2 g/m^2.

XG content was crucial in maximizing water absorption as a function of coating weight on the surface: to obtain a Cobb60 value under 10 g/m^2, a coating weight of 18 g/m^2 with 0.2 % XG, 15 g/m^2 with 0.4 % XG, and 10 g/m^2 with 0.8 % XG were needed (Fig. 12a). The effect is highlighted in Fig. 12b, which shows Cobb60 as a function of coating weight for samples obtained using the 4 µm bar. Similar and very low Cobb60 values of 3–4 g/m^2 were obtained with 0.8 % XG -thickened dispersion irrespective of the coating thickness. On the other hand, using 0.4 % XG resulted in a constant decrease in Cobb60 as coating weight increased, eventually reaching values similar to those obtained with 0.8 % XG. Using 0.2 % XG led to a similar trend as 0.4 % XG but with higher Cobb60 values.

We hypothesize that coating weight as regards water absorptiveness may be divided into two fractions: a) the effective fraction, due to the polymer in the film layer located on top of the pulp fibers network; b) the ineffective fraction, attributable to polymer chains that penetrate the pores of the fiber network. This latter portion is not continuous, and thus it is poorly effective in conferring barrier properties against liquid water. Low viscosity values of the dispersion result in easier penetration into the pores and increase the ineffective coating fraction in proportion to the total coating weight. Thus, the greater viscosity obtained with a higher thickener concentration (Table S4) is crucial for maximizing water resistance per weight of coating applied on paper. When a certain effective coating weight is obtained, as seems to already be the case for 0.8 % XG from 10 g/m^2 onwards, water absorption is minimized, and little reduction in Cobb60 takes place with further increases in coating weight.

When dispersions with low solid content (PLA15; solid content = 16 ± 3 wt%) were used, water absorptiveness values below 10 g/m^2 could not be obtained. A Cobb60 of 14 g/m^2 was reached at 15 g/m^2 of coating weight. Notice that 8 g/m^2 absorptiveness was instead obtained at the same coating weight with the high-solid dispersion with 0.4 % XG. This may be attributed to the lower viscosity (3.7 vs 15.5 Pa•s at 1 s^{-1} shear rate, Table S4) of the low-solid dispersion and to the higher content (2.5-fold) of hydrophilic XG.

Water absorption values have been previously reported for PLA coatings on paper obtained using various techniques. Two papers report

the values of classically solvent-borne semi-crystalline PLA coating: one used the Cobb120 index and reported values ranging from 12 to 0.2 g/m^2 for coating weights in the 3–90 g/m^2 range [11], while the other used the Cobb30 index and reported values of 9 to 3 g/m^2 for coating weights in the 6–9 g/m^2 range [12]; in both cases, water absorption constantly decreased with increasing coating weight. Electrosprayed solvent-borne semicrystalline coatings in the 3–8 g/m^2 range have been reported to have a Cobb120 index of 2 g/m^2, in this case not changing with coating weight [59]. The coatings we obtained differ from these experiments, not only in coating technique, but also for the presence of various additives (surfactants and thickener) and for the amorphous nature of the PLA used. Despite this, the values of 2–3 g/m^2 we obtained at 10–15 g/m^2 coating weight in the best formulations are quite similar to those observed by the various authors. Indeed, a study on the effect of the addition of PEG as plasticizer in PLA coatings found that it did not change water absorption up to 10 % weight content and then had a moderate hydrophilic effect with increasing content [60]. This finding is in agreement with our results. In fact, the hydrophilic components in the coatings are PEG and XG. The former is present in approximately 10 % by weight and the latter in 0.5–2 % by weight, and these combinations were found to not have a significant hydrophilic effect on the overall coating. Thus, the waterborne dispersion technique can substitute the use of harmful organic solvents successfully while achieving similar results. Compared to recently reported waterborne biodegradable coatings obtained with other polyesters, the water resistance performance of PLA coatings was superior to that of both PBS and PHBV, despite these polymers being used in much thicker layers (> 30 μm) [20,21].

Barrier properties against water vapor were also analyzed for coated paper by testing the WVTR of two selected samples, both obtained with PLA40 and 0.8 % XG. The samples have a coating weight of 10 and 15 g/m^2, corresponding to samples 2 × 4 and 4 × 4 illustrated in Fig. 12a. These tests were carried out at 22 °C and 51 % relative humidity, aiming to emulate normal indoor conditions. The values of WVTR (Table 2) show that the PLA coating strongly reduces the WVTR of paper, by 60 % and 75 % when 10 and 15 g/m^2 coating weights are applied, respectively. This value may be normalized by thickness and water vapor pressure for easier comparison to other materials to obtain the water vapor permeability (WVP) of the coated paper, which was reduced by 56 and 70 % respectively compared to pristine paper.

The coated paper could be considered a double-layer material consisting of a paper layer and a PLA layer on top. The overall permeability of such material in this case may be determined from the individual layer permeabilities using the following formula:

$$WVP = \frac{L}{\frac{L_{paper}}{WVP_{paper}} + \frac{L_{PLA}}{WVP_{PLA}}} \quad (5)$$

where L_x represents the thickness of layer x and WVP_x is its water vapor permeability. Since all other values were measured, this equation can be utilized to calculate the water vapor permeability (WVP_{PLA}) of the PLA coating layer which was found to be in the range of 0.8–1.2 × 10^6 g/(m·days·Pa) (Table 2). The water vapor permeability (WVP) of PLA has been reported to range from 1.4 to 1.6 × 10^6 g/(m·days·Pa) under similar humidity and temperature conditions to our tests [61]. The values of WVP_{PLA} obtained from the two samples were somewhat lower than this reference. This is likely because the actual structure of the multilayer material obtained by coating the paper using the waterborne technique is not simply a paper layer overlaid by a PLA one but includes a transitional layer of paper with pores filled by the polymer. Thus, the actual effective thickness of the PLA layer is probably higher than the one that may be directly measured by SEM and was used for calculation. This is confirmed by the WVP_{PLA} value of the 15 g/m^2 sample being higher and close to the theoretical one, as the transitional layer has comparatively less impact as the PLA layer gets thicker. The PLA layer is also not composed of pure PLA, but it is a blend including two other main components, the ELE surfactant and the XG thickener. However, these components are both hydrophilic, so it would be surprising if they conferred higher water vapor barrier properties to the material. Thus, the coated paper can overall be conceptualized as a two-layer paper-PLA material, with barrier properties to water vapor directly derived from the properties of the layers.

While a marked improvement in WVTR was achieved compared to pristine paper, due to the inherently mediocre water vapor barrier properties of PLA compared to fossil-based polymers (for example, the commonly used LDPE has a WVP more than an order of magnitude lower than PLA [62]), the water vapor barrier properties of the coated paper are still inadequate for applications where a low WVTR is needed, and more appropriate for packaging where moderate water transmission is desired. This is consistent with the results obtained by other researchers on paper coated with PLA [11,29].

The surface energy of the PLA-coated paper was measured using the Dyne Test ink method, and the values measured ranged between 42 and 56 dyne/cm (Table S6). This range of surface energy values is higher than that of neat PLA materials (38 dyne/cm) [63], a variation which is attributed to the presence of surfactants on the surface that are more polar than PLA itself. As the coated paper thus has higher wettability by polar formulations, such as most inks and paints, compared to a pure PLA material, it is expected to be more easily printed on and dyed, as well as being somewhat less hydrophobic than paper coated with PLA by extrusion [64]. Indeed, the surface energy of our PLA coating is similar to that of PLA modified for this purpose by plasma treatment [65].

In order to determine the effect of PLA coating on the recyclability of the coated paper, we carried out preliminary repulpability tests. In one test, we observed the time it took for a paper sample, pre-soaked in cold water for 72 h, to be completely reduced to pulp by agitation at 40 °C. Pristine paper, as a reference, was pulped in 1 h. Three coated papers with coating weights of 10, 12, and 15 g/m^2 (PLA40, 0.8 % XG, entries 2 × 4,3 × 4, and 4 × 4 in Fig. 12a) were tested: the 10 g/m^2 sample was pulped in 5 h while the others were both pulped overnight (between 8 and 18 h). These preliminary tests thus indicate that even if slower, repulpability of the coated paper is possible. In another test, the rate of rejects (pieces of sample unable to pass through a sieve) to overall coated paper weight was measured after 2 h of stirring at 40 °C. The reject rate for the same three samples after this time was 15 %, 14 %, and 32 % in increasing order of coating weight. For comparison, Zhang and colleagues found a 21 % reject rate for the repulpability of PLA-coated paper, thus in a similar range albeit using a somewhat different

Table 2
Water vapor barrier properties of PLA40-coated and uncoated paper sheets were recorded at 22 °C and 51 % relative humidity.

Coating weight	Thickness (μm)[a]	L_{PLA} (μm)[b]	WVTR (g/(m^2×days))	WVP × 10^6 (g/(m×days×Pa))	WVP_{PLA} × 10^6 (g/(m×days×Pa))[c]
Uncoated paper	98 ± 2	–	310 ± 20	22 ± 1	–
10 g/m^2	104 ± 3	5.1 ± 0.3	127 ± 2	9.7 ± 0.2	0.81 ± 0.07
15 g/m^2	110 ± 3	14 ± 1	83 ± 3	6.7 ± 0.3	1.2 ± 0.1

[a] Paper + coating as measured by micrometre.
[b] Measured on SEM images (Fig. S6).
[c] $WVP_{PLA} = (WVP \bullet WVP_{paper} \bullet L_{PLA})/(WVP_{paper} \bullet L - WVP \bullet L_{paper})$.

method [66]. Overall, this data confirms the importance of limiting coating weight to achieve easier recycling and indicates significantly better repulping for coating weights below 15 g/m^2.

4. Conclusions

In this study, we have explored the utilization of PEG-PLA-PEG triblock copolymers (ELE) as surfactants to fabricate waterborne PLA dispersions. To achieve this, we employed an oil-in-water ultrasonication method previously utilized with commercial surfactants. The dispersions produced through this method, using 2–3 % ELE, exhibited particle sizes ranging from 400 to 700 nm and solid contents of 13–18 wt %. While they remained stable in the short term, they exhibited increasing phase separation beyond 2–8 weeks from preparation. However, the addition of SDS as a co-surfactant in minor quantities (0.05–0.1 %) with similar solid content proved effective in reducing particle size to below 300 nm and enhancing the long-term stability of the dispersions. Specifically, dispersions containing 3 % ELE and 0.1 % SDS retained over 90 % of dispersed solids after 6 months in storage. The hydrolytic stability of PLA in waterborne formulations stored at 4 °C was observed to proceed constantly but slowly via hydrolysis for the first 7.5 months, with a loss of around 2 % mass per month of high-molecular-weight polymer. Subsequently, there was an acceleration in hydrolytic degradation. All formulations with an SDS content lower than 0.4 % could be cast into transparent films at 60 °C, displaying glass transition temperatures below 40 °C and minimum film formation temperatures in the 38–49 °C temperature range. Formulations with solid content above 40 wt% could be achieved by concentrating the original dispersions when at least 3 % ELE and 0.05 % SDS were used, with minimal change in particle size and dispersion stability. This represents the first report in the scientific literature of the preparation of such high solid content for PLA dispersions, similar to some industrial formulations but with significantly reduced particle size.

Dispersions using 3 % ELE and 0.05 % SDS as surfactants were thickened using XG, reaching viscosities of 14–15 Pa s (at a shear rate of 1 s^{-1}) and 36 Pa s with 0.2–0.4 % and 0.8 % of XG, respectively. All formulations exhibited shear-thinning behavior, and the viscosity plots could be well-fitted by power-law or Cross models. Once applied as a coating on paper, the most viscous formulation was found to be the most effective in reducing water absorption even at low coating weights (~10 g/m^2) due to its reduced capability to penetrate into the paper pores. Despite some penetration within the pores observed with all formulations, very good adhesion of the coating to the paper substrate was achieved, from which it could not be mechanically detached. Using 40 wt% PLA dispersion with 0.8 % XG as a thickener, a Cobb60 value of 3–4 g/m^2 was obtained at 10–15 g/m^2 coating weight, representing a > 95 % reduction from the original paper, similar to what may be achieved using organic solvents. The water vapor transmission rate (WVTR) of paper was reduced by 75 % with a 15 g/m^2 coating weight, corresponding to the reduction expected by the PLA layer based on literature data, indicating no or negligible effect of the additives (PEG blocks in ELE and XG). The surface energy of the coating was higher than that of PLA itself (42–56 dyne/cm instead of 38) due to a greater presence of polar groups on the surface, likely caused by the surfactant additives. Such a surface is thus less hydrophobic and more easily dyable compared to PLA. Paper coated with 10–15 g/m^2 of PLA could be repulped, although it required more time than pristine paper. Furthermore, the ease of repulpability decreased with the thickness of the PLA coating layer.

Funding

This activity was partially supported by the University of Ferrara trough FAR 2022, FAR 2023 and by Italian MUR – trough the project "CURSA Industria 4.0 - PROCESSI DI DIGITALIZZAZIONE DELLE PUBBLICHE AMMINISTRAZIONI E DI AMBITI PRODUTTIVI SECONDO LE LINEE GUIDA DEL PROGRAMMA INDUSTRIA 4.0" - CUP Number B53C21001630001.

CRediT authorship contribution statement

Matteo Calosi: Writing – original draft, Investigation. **Andrea D'Iorio:** Investigation. **Elena Buratti:** Writing – review & editing, Visualization, Data curation. **Rita Cortesi:** Supervision. **Silvia Franco:** Investigation, Formal analysis. **Roberta Angelini:** Supervision, Formal analysis. **Monica Bertoldo:** Writing – review & editing, Supervision, Funding acquisition, Conceptualization.

Declaration of competing interest

The authors declare no competing interests.

Data availability

Data will be made available on request.

Acknowledgement

Dr. Viviana Conti from NatureWorks is kindly acknowledged for providing PLA.

Appendix A. Supplementary data

The supporting information file contains the following data: Fitting of viscosity plots; ^{1}H NMR spectrum of ELE surfactant in $CDCl_3$; picture of a film cast from ELE3.0-SDS5 at 60 °C; pictures of film samples, detached from the aluminum plates, of the MFFT measurements of ELE3.0-SDS5; DSC thermograms of ELE surfactant and PLA film cast at 60 °C from ELE3.0 dispersion; viscosity as a function of shear rate for water solutions of xanthan gum (XG); coating thickness measurements in SEM images; intensity distribution and polydispersity by DLS analysis for PLA waterborne dispersions; optical transmittance at 600 nm for films cast at 60 °C from PLA dispersions; apparent glass transition temperatures by DSC analysis of films cast at 60 °C from waterborne PLA; parameters from the Power law (Eq. (1)) and Cross (Eq. (2)) fits to the experimental viscosity plots; sample list and water absorption properties of paper sheets coated with PLA15 and PLA40 thickened with XG; surface energy data of coated paper. Supplementary data to this article can be found online at doi:https://doi.org/10.1016/j.porgcoat.2024.108541.

References

[1] P. Tyagi, K.S. Salem, M.A. Hubbe, L. Pal, Advances in barrier coatings and film technologies for achieving sustainable packaging of food products – a review, Trends Food Sci. Technol. 115 (2021) 461–485, https://doi.org/10.1016/j.tifs.2021.06.036.
[2] J. De Temmerman, I. Vermeir, H. Slabbinck, Eating out of paper versus plastic: the effect of packaging material on consumption, Food Qual. Prefer. 112 (2023) 105023, https://doi.org/10.1016/j.foodqual.2023.105023.
[3] P.K. Kunam, D. Ramakanth, K. Akhila, K.K. Gaikwad, Bio-based materials for barrier coatings on paper packaging, Biomass Convers. Biorefinery (2022), https://doi.org/10.1007/s13399-022-03241-2.
[4] K. Khwaldia, E. Arab-Tehrany, S. Desobry, Biopolymer coatings on paper packaging materials, Compr. Rev. Food Sci. Food Saf. 9 (2010) 82–91, https://doi.org/10.1111/j.1541-4337.2009.00095.x.
[5] S. Basak, M.S. Dangate, S. Samy, Oil- and water-resistant paper coatings: a review, Prog. Org. Coat. 186 (2024) 107938, https://doi.org/10.1016/j.porgcoat.2023.107938.
[6] P. Nechita, M. Roman (Iana-Roman), Review on polysaccharides used in coatings for food packaging papers, Coatings 10 (2020) 566, https://doi.org/10.3390/coatings10060566.
[7] Z.A. Nur Hanani, Surface properties of biodegradable polymers for food packaging, in: T.J. Gutiérrez (Ed.), Polym, Food Appl., Springer International Publishing, Cham, 2018, pp. 131–147, https://doi.org/10.1007/978-3-319-94625-2_6.
[8] R. Auras, B. Harte, S. Selke, An overview of polylactides as packaging materials, Macromol. Biosci. 4 (2004) 835–864, https://doi.org/10.1002/mabi.200400043.

[9] S. Mohan, K. Panneerselvam, A short review on mechanical and barrier properties of polylactic acid-based films, Mater. Today Proc. 56 (2022) 3241–3246, https://doi.org/10.1016/j.matpr.2021.09.375.

[10] M. Mujtaba, J. Lipponen, M. Ojanen, S. Puttonen, H. Vaittinen, Trends and challenges in the development of bio-based barrier coating materials for paper/cardboard food packaging; a review, Sci. Total Environ. 851 (2022) 158328, https://doi.org/10.1016/j.scitotenv.2022.158328.

[11] J.-W. Rhim, J.-H. Kim, Properties of poly(lactide)-coated paperboard for the use of 1-way paper cup, J. Food Sci. 74 (2009) E105–E111, https://doi.org/10.1111/j.1750-3841.2009.01073.x.

[12] S. N, A.K. S, P. A, G. S, Studies on semi-crystalline poly lactic acid (PLA) as a hydrophobic coating material on kraft paper for imparting barrier properties in coated abrasive applications, Prog. Org. Coat. 145 (2020) 105682, https://doi.org/10.1016/j.porgcoat.2020.105682.

[13] S. Marano, E. Laudadio, C. Minnelli, P. Stipa, Tailoring the barrier properties of PLA: a state-of-the-art review for food packaging applications, Polymers 14 (2022) 1626, https://doi.org/10.3390/polym14081626.

[14] M. Karamanlioglu, R. Preziosi, G.D. Robson, Abiotic and biotic environmental degradation of the bioplastic polymer poly(lactic acid): a review, Polym. Degrad. Stab. 137 (2017) 122–130, https://doi.org/10.1016/j.polymdegradstab.2017.01.009.

[15] CPI publishes revised Design for Recyclability Guidelines. https://paper.org.uk/CPI/CPI/Content/News/Press-Releases/2022/CPI-publishes-revised-Design-for-Recyclability-Guidelines.aspx. (Accessed 20 December 2023) (n.d.).

[16] S. Sängerlaub, M. Brüggemann, N. Rodler, V. Jost, K.D. Bauer, Extrusion coating of paper with poly(3-hydroxybutyrate-co-3-hydroxyvalerate) (PHBV)—packaging related functional properties, Coatings 9 (2019) 457, https://doi.org/10.3390/coatings9070457.

[17] B.A. Morris, Understanding why adhesion in extrusion coating decreases with diminishing coating thickness, J. Plast. Film Sheeting 24 (2008) 53–88, https://doi.org/10.1177/8756087908089486.

[18] A. Shankar, A.M. Ak, R. Narayan, A. Chakrabarty, Emulsion polymerized styrene acrylic/nanocellulose composite coating to improve the strength and hydrophobicity of kraft paper, Prog. Org. Coat. 182 (2023) 107634, https://doi.org/10.1016/j.porgcoat.2023.107634.

[19] Z. Aguirreurreta, J.C. de la Cal, J.R. Leiza, Preparation of high solids content waterborne acrylic coatings using polymerizable surfactants to improve water sensitivity, Prog. Org. Coat. 112 (2017) 200–209, https://doi.org/10.1016/j.porgcoat.2017.06.028.

[20] S.S. Hamdani, H. Emch, J. Isherwood, A. Khan, V. Kumar, A. Alford, I. Wyman, R. Sharma, P. Mayekar, A. Bher, R. Auras, M. Rabnawaz, Waterborne poly (butylene succinate)-coated paper for sustainable packaging applications, ACS Appl. Polym. Mater. 5 (2023) 7705–7717, https://doi.org/10.1021/acsapm.3c00846.

[21] K. Pieters, T.H. Mekonnen, Stable aqueous dispersions of poly(3-hydroxybutyrate-co-3-hydroxyvalerate) (PHBV) polymer for barrier paper coating, Prog. Org. Coat. 187 (2024) 108101, https://doi.org/10.1016/j.porgcoat.2023.108101.

[22] Polylactide resin emulsions - LANDY PL Series. https://www.miyoshi-yushi.co.jp/en/business-information/pdf/06_landyPL_en202210.pdf, 2022. (Accessed 25 July 2023).

[23] S. Yamamoto, Y. Kasukabe, C. Yamashita, T. Tanaka, N. Nagatani, Polylactic acid-containing aqueous dispersion, US10987299B2. https://patents.google.com/patent/US10987299B2/en, 2021. (Accessed 18 April 2023).

[24] S.J. Hipps, H. Cai, E.R. Gay, T.M. Collins, J.B. Homoelle, Aqueous-based hydrolytically stable dispersion of a biodegradable polymer, WO2017151595A1. https://patents.google.com/patent/WO2017151595A1/en, 2017. (Accessed 18 April 2023).

[25] D. Bandera, V.R. Meyer, D. Prevost, T. Zimmermann, L.F. Boesel, Polylactide/montmorillonite hybrid latex as a barrier coating for paper applications, Polymers 8 (2016) 75, https://doi.org/10.3390/polym8030075.

[26] G. Belletti, S. Buoso, L. Ricci, A. Guillem-Ortiz, A. Aragón-Gutiérrez, O. Bortolini, M. Bertoldo, Preparations of poly(lactic acid) dispersions in water for coating applications, Polymers 13 (2021) 2767, https://doi.org/10.3390/polym13162767.

[27] S. Buoso, G. Belletti, D. Ragno, V. Castelvetro, M. Bertoldo, Rheological response of polylactic acid dispersions in water with xanthan gum, ACS Omega 7 (2022) 12536–12548, https://doi.org/10.1021/acsomega.1c05382.

[28] G. Belletti, G. Ronconi, V. Mazzanti, E. Buratti, L. Marchi, G. Sotgiu, M. Calosi, F. Mollica, M. Bertoldo, Morphology and mechanical properties of poly(vinyl alcohol)/poly(lactic acid) blend films prepared from aqueous dispersions, Macromol. Mater. Eng. 309 (2024) 2300237, https://doi.org/10.1002/mame.202300237.

[29] C. Abdenour, M. Eesaee, C. Stuppa, B. Chabot, S. Barnabé, J. Bley, B. Tolnai, N. Guy, P. Nguyen-Tri, Water vapor and air barrier performance of sustainable paper coatings based on PLA and xanthan gum, Mater. Today Commun. 36 (2023) 106626, https://doi.org/10.1016/j.mtcomm.2023.106626.

[30] S. Farah, D.G. Anderson, R. Langer, Physical and mechanical properties of PLA, and their functions in widespread applications — a comprehensive review, Adv. Drug Deliv. Rev. 107 (2016) 367–392, https://doi.org/10.1016/j.addr.2016.06.012.

[31] D. Cohn, H. Younes, Biodegradable PEO/PLA block copolymers, J. Biomed. Mater. Res. 22 (1988) 993–1009, https://doi.org/10.1002/jbm.820221104.

[32] S. Miyamoto, K. Takaoka, T. Okada, H. Yoshikawa, J. Hashimoto, S. Suzuki, K. Ono, Polylactic acid-polyethylene glycol block copolymer: a new biodegradable synthetic carrier for bone morphogenetic protein, Clin. Orthop. 294 (1993) 333–343, https://doi.org/10.1097/00003086-199309000-00050.

[33] D.R. Perinelli, M. Cespi, G. Bonacucina, G.F. Palmieri, PEGylated polylactide (PLA) and poly (lactic-co-glycolic acid) (PLGA) copolymers for the design of drug delivery systems, J. Pharm. Investig. 49 (2019) 443–458, https://doi.org/10.1007/s40005-019-00442-2.

[34] A. Chaos, A. Sangroniz, J. Fernández, J. del Río, M. Iriarte, J.R. Sarasua, A. Etxeberria, Plasticization of poly(lactide) with poly(ethylene glycol): low weight plasticizer vs triblock copolymers. Effect on free volume and barrier properties, J. Appl. Polym. Sci. 137 (2020) 48868, https://doi.org/10.1002/app.48868.

[35] W. Yodthong Baimark, N. Prakymoramas Rungseesantivanon, Improvement in crystallization and toughness of poly(L-lactide) by melt blending with poly(L-lactide)-b-polyethylene glycol-b-poly(L-lactide) in the presence of chain extender, Polym. Sci. Ser. A 63 (2021) S34–S45, https://doi.org/10.1134/S0965545X22030051.

[36] E.J. Rodriguez, B. Marcos, M.A. Huneault, Hydrolysis of polylactide in aqueous media, J. Appl. Polym. Sci. 133 (2016), https://doi.org/10.1002/app.44152.

[37] A. Porfyris, S. Vasilakos, C. Zotiadis, C. Papaspyrides, K. Moser, L. Van der Schueren, G. Buyle, S. Pavlidou, S. Vouyiouka, Accelerated ageing and hydrolytic stabilization of poly(lactic acid) (PLA) under humidity and temperature conditioning, Polym. Test. 68 (2018) 315–332, https://doi.org/10.1016/j.polymertesting.2018.04.018.

[38] W. Limsukon, R. Auras, S. Selke, Hydrolytic degradation and lifetime prediction of poly(lactic acid) modified with a multifunctional epoxy-based chain extender, Polym. Test. 80 (2019) 106108, https://doi.org/10.1016/j.polymertesting.2019.106108.

[39] B. Jeong, Y.H. Bae, D.S. Lee, S.W. Kim, Biodegradable block copolymers as injectable drug-delivery systems, Nature 388 (1997) 860–862, https://doi.org/10.1038/42218.

[40] L. Bollenbach, J. Buske, K. Mäder, P. Garidel, Poloxamer 188 as surfactant in biological formulations – an alternative for polysorbate 20/80? Int. J. Pharm. 620 (2022) 121706 https://doi.org/10.1016/j.ijpharm.2022.121706.

[41] X. Guo, Z. Rong, X. Ying, Calculation of hydrophile–lipophile balance for polyethoxylated surfactants by group contribution method, J. Colloid Interface Sci. 298 (2006) 441–450, https://doi.org/10.1016/j.jcis.2005.12.009.

[42] A.J.P. van Zyl, D. de Wet-Roos, R.D. Sanderson, B. Klumperman, The role of surfactant in controlling particle size and stability in the miniemulsion polymerization of polymeric nanocapsules, Eur. Polym. J. 40 (2004) 2717–2725, https://doi.org/10.1016/j.eurpolymj.2004.07.021.

[43] L.L. Hecht, C. Wagner, K. Landfester, H.P. Schuchmann, Surfactant concentration regime in miniemulsion polymerization for the formation of MMA nanodroplets by high-pressure homogenization, Langmuir 27 (2011) 2279–2285, https://doi.org/10.1021/la104480s.

[44] W. McPhee, K.C. Tam, R. Pelton, Poly(N-isopropylacrylamide) latices prepared with sodium dodecyl sulfate, J. Colloid Interface Sci. 156 (1993) 24–30, https://doi.org/10.1006/jcis.1993.1075.

[45] J.R. Rocca-Smith, O. Whyte, C.-H. Brachais, D. Champion, F. Piasente, E. Marcuzzo, A. Sensidoni, F. Debeaufort, T. Karbowiak, Beyond biodegradability of poly(lactic acid): physical and chemical stability in humid environments, ACS Sustain. Chem. Eng. 5 (2017) 2751–2762, https://doi.org/10.1021/acssuschemeng.6b03088.

[46] A. Kumar, C.K. Dixit, 3 - methods for characterization of nanoparticles, in: S. Nimesh, R. Chandra, N. Gupta (Eds.), Adv. Nanomedicine Deliv. Ther, Nucleic Acids, Woodhead Publishing, 2017, pp. 43–58, https://doi.org/10.1016/B978-0-08-100557-6.00003-1.

[47] A. Toussaint, M. De Wilde, F. Molenaar, J. Mulvihill, Calculation of Tg and MFFT depression due to added coalescing agents, Prog. Org. Coat. 30 (1997) 179–184, https://doi.org/10.1016/S0300-9440(96)00685-6.

[48] S.M. Dron, S.J. Bohorquez, D. Mestach, M. Paulis, Reducing the amount of coalescing aid in high performance waterborne polymeric coatings, Eur. Polym. J. 170 (2022) 111175, https://doi.org/10.1016/j.eurpolymj.2022.111175.

[49] J.W. Nicholson, Waterborne coatings, in: A.D. Wilson, J.W. Nicholson, H.J. Prosser (Eds.), Surf. Coatings—2, Springer Netherlands, Dordrecht, 1988, pp. 1–38, https://doi.org/10.1007/978-94-009-1351-6_1.

[50] T.F. Protzman, G.L. Brown, An apparatus for the determination of the minimum film temperature of polymer emulsions, J. Appl. Polym. Sci. 4 (1960) 81–85, https://doi.org/10.1002/app.1960.070041012.

[51] C.L. Zhao, Y. Holl, T. Pith, M. Lambla, FTIR-ATR spectroscopic determination of the distribution of surfactants in latex films, Colloid Polym. Sci. 265 (1987) 823–829, https://doi.org/10.1007/BF01418459.

[52] D. Scalarone, M. Lazzari, V. Castelvetro, O. Chiantore, Surface monitoring of surfactant phase separation and stability in waterborne acrylic coatings, ACS Publ. (2007), https://doi.org/10.1021/cm0714077.

[53] G.H. Xu, J. Dong, S.J. Severtson, C.J. Houtman, L.E. Gwin, Modifications of surfactant distributions and surface morphologies in latex films due to moisture exposure, J. Phys. Chem. B 113 (2009) 10189–10195, https://doi.org/10.1021/jp902716b.

[54] D.F.S. Petri, Xanthan gum: a versatile biopolymer for biomedical and technological applications, J. Appl. Polym. Sci. 132 (2015), https://doi.org/10.1002/app.42035.

[55] J. Borch, Thermodynamics of polymer-paper adhesion: a review, J. Adhes. Sci. Technol. 5 (1991) 523–541, https://doi.org/10.1163/156856191X00729.

[56] J. Kuusipalo, A. Savolainen, Adhesion phenomena in (co)extrusion coating of paper and paperboard, J. Adhes. Sci. Technol. (1997), https://doi.org/10.1163/156856197X00877.

[57] B. Zhao, R. Pelton, V. Bartzoka, Peeling pressure sensitive tape from paper, in: Adv. Pap. Sci. Technol. Trans. 13th Fundam. Res. Symp. Camb, Fundamental Research Committee, Manchester, 2005, pp. 827–850. https://bioresources.cnr.ncsu.edu/wp-content/uploads/2020/07/2005.2.827.pdf. (Accessed 7 May 2024).

[58] E. Alanen, Adhesion Characterization of Extrusion Coated Paperboards, Tampere University, 2023. https://trepo.tuni.fi/bitstream/handle/10024/146535/AlanenElli.pdf?sequence=2. (Accessed 7 May 2024) (Masters Thesis).
[59] T. Archaviboonyobul, T. Jinkarn, S. Sane, S. Chariyachotilert, S. Kongcharoenkiat, Water resistance and barrier properties improvement of paperboard by poly(lactic acid) electrospraying, Packag. Technol. Sci. 27 (2014) 341–352, https://doi.org/10.1002/pts.2034.
[60] N. Sundar, S.J. Stanley, S.A. Kumar, P. Keerthana, G.A. Kumar, Development of dual purpose, industrially important PLA–PEG based coated abrasives and packaging materials, J. Appl. Polym. Sci. 138 (2021) 50495, https://doi.org/10.1002/app.50495.
[61] R.A. Auras, B. Harte, S. Selke, R. Hernandez, Mechanical, physical, and barrier properties of poly(lactide) films, J. Plast. Film Sheeting 19 (2003) 123–135, https://doi.org/10.1177/8756087903039702.
[62] M.E. González-López, S. de J. Calva-Estrada, M.S. Gradilla-Hernández, P. Barajas-Álvarez, Current trends in biopolymers for food packaging: a review, Front. Sustain. Food Syst. 7 (2023), https://doi.org/10.3389/fsufs.2023.1225371 (accessed January 26, 2024).
[63] X. Rong, M. Keif, A study of PLA printability with flexography, in: 59th Annu. Tech. Assoc. Graph. Arts Tech. Conf. Proc. Pittsburgh PA, 2007. https://digitalcommons.calpoly.edu/grc_fac/16.
[64] C. Aydemir, B.N. Altay, M. Akyol, Surface analysis of polymer films for wettability and ink adhesion, Color. Res. Appl. 46 (2021) 489–499, https://doi.org/10.1002/col.22579.
[65] A. Jordá-Vilaplana, V. Fombuena, D. García-García, M.D. Samper, L. Sánchez-Nácher, Surface modification of polylactic acid (PLA) by air atmospheric plasma treatment, Eur. Polym. J. 58 (2014) 23–33, https://doi.org/10.1016/j.eurpolymj.2014.06.002.
[66] H. Zhang, D. Bussini, M. Hortal, G. Elegir, J. Mendes, M. Jordá Beneyto, PLA coated paper containing active inorganic nanoparticles: material characterization and fate of nanoparticles in the paper recycling process, Waste Manag. 52 (2016) 339–345, https://doi.org/10.1016/j.wasman.2016.03.045.